DEPARTMENT OF PHYSICS

RESEARCH REPORT NUMBER 68-2

PENETRATION AND INTERACTION OF PROTONS WITH MATTER

PART I. THEORETICAL STUDIES USING MONTE CARLO TECHNIQUES

Edited
by

MARTIN LEIMDORFER
and
GEORGE W. CRAWFORD

Sponsored by

National Aeronautics and Space Administration
Research Grant NsG 708

Principal Investigator: George W. Crawford
Report Period: June 1, 1964 through August 31, 1968

August, 1968

SOUTHERN METHODIST UNIVERSITY
DALLAS, TEXAS 75222

SOUTHERN METHODIST UNIVERSITY

DEPARTMENT OF PHYSICS

RESEARCH REPORT NUMBER 68-2

PENETRATION AND INTERACTION OF PROTONS WITH MATTER

PART I: THEORETICAL STUDIES USING MONTE CARLO TECHNIQUES

CONTENTS

CHAPTER 1

INTRODUCTION TO THE PROPER 3B SYSTEM

by George W. Crawford

The PROPER 3B system is described in detail in Chapter 4 of this report and in Part IA: Instruction Manual for User of Monte Carlo Proton Transport Program, Grant NsG 708 Report dated September, 1967. The system is a flexible combination of computer programs which may be used to solve a number of different problems, involving nucleon transport and interaction.

The user may select the type or combination of types of nucleon comprising the incident beam; the energy, energy spectrum and direction of the particle flux; and the type of matter, its size, shape and orientation through which the nucleons are traveling. The program as delivered to NASA contains nuclear interaction data for protons and neutrons at energies up to 400 MeV. The program can be expanded to handle higher energy particles as data become available.

For a given source flux and target, the program calculates the energy, direction and space distributions of nucleons and neutrons leaving all of the faces of the selected volume. It also provides a full history of each primary particle and its secondaries inside the chosen volume. The combination of these are used to determine the energy absorbed by the matter in the volume or any smaller, enclosed portion of the volume. Dose is calculated as the differences between the sum of the energies of all the directly and indirectly ionizing particles which have entered the volume and the sum of the energies of all those which have left it, minus the energy equivalent of any increase in rest mass that took place in nuclear reactions within the volume.

The particle flux, both primary and secondary, leaving any one of the faces of the original volume may be used as the source flux entering a new volume. This new volume may be of any material (for which the user can supply the required data) and any shape or size. Thus the user may surround the original volume with as many different materials and may carry the flux through as many different bodies as desired.

The flexibility of the source, target and output programs permits this system to be used for many space radiation environments of interest to NASA. These include dosimetry and shielding applications. Some suggested applications are the following:

1. Estimation of the radiation hazard to an astronaut in any assumed proton radiation environment. This is to be accomplished by calculating the dose (-rate), depth dose (-rate) distribution and the dose (-rate) to selected organs in an actual man for any anticipated radiation environment.
2. The surface dose and depth dose distribution will be different at different parts of the body of the astronaut. The inherent property of the geometry and mass distribution characteristics of the space vehicle and space suits will produce a non-uniform exposure. This program permits selection of any size or shape of entrance zone. By using a "patchwork quilt" of zones, each having a different initial radiation environment, the surface dose and depth dose distribution so calculated is a better determination of the hazard.
3. The non-uniform distribution of the parts of the body, such as critical tissues and organs, further modifies an existing diversity of radiation environment. Also these organs are located under varying levels of shielding (flesh, bone, fat) for each astronaut. The program permits a depth dose distribution

to be calculated which represents the actual dimensions of skin, flesh, bone, and other tissues for each individual. Hence the dose calculated at the critical organ for a given radiation environment would be correct for the individual receiving the dose. The values obtained by using an "average" man are only estimates.

4. Utilization of detector-dosimeter readings as telemetered to earth to calculate the proton dose, depth dose distribution and dose to selected organs during an actual space radiation exposure.

5. Correlation of dosimeter response to dose and depth dose distributions for biological experiments at any proton accelerator facility.

6. To duplicate mathematically the experiment conducted at any proton accelerator facility. For example, PROPER 3B was used to plan and to interpret the proton transport data required to study the characteristics of semiconductor detector-dosimeters in Grant NsG 708.

7. The system can also be used to determine the best design for a dosimeter under a given radiation condition. The dosimeter can be of any material and could be "passive" (measurement made long after exposure) or active (data taken during exposure). It is applicable to a study of tissue equivalence of plastic covered dosimeters.

8. Shielding problems of many different kinds may be studied using PROPER 3B.

Even though the present system is a versatile tool for studying the transport ofnucleons at energies below 400 MeV, it is obvious that a further increase in the capability of the program is desireable. Some lines of immediate extension are listed. *

1. Extending the energy range upwards. The work by H. Bertini at ORNL of extending the intra-nuclear cascade calculations to 2 GeV is now available. This addition will require the considerations of pions. The pion transport can be simulated in complete analogy with PROTOS 3 and SUPER B methods. Pion decay, giving rise to muons, is also a straight-forward extension.

2. Adding electron transport codes to the system.

3. Including gamma ray and x-ray transport. Existing programs can be adapted to the PROPER 3B system. Secondary gamma production data would have to be compiled.

4. Introduction of a more flexible general geometry for multi-medium problems as storage facilities increase in the computer.

In Chapter 1-2, the concept of linear stopping power is developed and the Bethe-Bloch equation 2-29 is derived. This equation is required in the Monte Carlo transport code developed in Chapter 1-3 for one part of the complex collision problems. The Monte Carlo code is the key program of the flexible PROPER 3B system described in Chapter 1-4. Chapters 1-5, 1-6, and 1-7 describe specific applications of the system. Part II is devoted to the measurement of the mean ionization potential, I, and the shell corrections for elements and compounds. These values are required for proper usage of PROTOS. The Monte Carlo program is used to duplicate the experimental conditions in a mathematical sense. The program was also used to determine the energy required to create an electron-hole pair in silicon as part of the detector-dosimeter study.

* For further information concerning extensions of PROPER 3B, contact
Dr. Martin Leimdorfer, President

Industri-Matematik AB

DE GEERSGATAN 8

Stockholm No.

Sweden.

CHAPTER 2

LINEAR STOPPING POWER

by Danny R. Dixon

INTRODUCTION

The interactions of energetic particles with solids have been used extensively to study both the properties of atomic structure as well as the properties of ionizing radiation. Work of this nature involves accurate and precise determination of the energy and momentum of the radiation.

A generally accepted concept is that nucleons (protons and heavier charged particles) traverse matter on an approximately straight path (1). These nucleons dissipate their energy primarily through a multitude of inelastic collisions with atomic electrons. The rate of average energy loss as a function of the nucleon energy is the stopping power of the material. The range of a particle is its penetration into a given material. This penetration depends chiefly on the average energy loss resulting from the nucleon electron collisions.

The key parameter in the derivation of a stopping power equation is the mean excitation energy, I, of the material. However, it is also necessary to take into account the contributions of such factors as shell corrections (2), density effects, and small angle scatterings (3).

Leimdorfer (4) has incorporated the stopping power expression for linear energy loss into a Monte Carlo nucleon transport program. This program includes the interaction of the nucleon with the free and bound atomic electrons, small angle scattering, large angle Rutherford scattering, and nuclear interactions.

THEORY

Consider the interaction of an incident charged particle passing through an absorber. If the incident particle travels a distance ds in the absorber of N atoms/cm^3 and Z electrons/atom, then the expectation value for the energy loss per unit path length, dT/ds, is given by

$$\frac{dT}{ds} = NZ \int_{Q_{min}}^{Q_{max}} Q \, d\sigma \qquad \text{ergs/cm}, \tag{2-1}$$

where Q represents the energy transfer, and σ represents the differential cross section $\Phi(Q)\, dQ$, whether the theory is classical non-relativistic, classical relativistic, or quantum mechanical. Hence, Eq. (1) can be written in the form

$$\frac{dT}{ds} = NZ \int_{Q_{min}}^{Q_{max}} Q \, \Phi(Q) \, dQ \qquad \text{ergs/cm}. \tag{2-2}$$

Now the problem is reduced to the question of evaluating $\Phi(Q)$, Q_{max} and Q_{min}.

Bohr's Classical Theory

Assume that the binding energy of each electron in the absorber is negligible in comparison to the kinetic energy it receives in the collision. The problem then reduces to a two-body, elastic coulomb scattering.

An incident particle (mass M, charge ze, velocity V, kinetic energy $T = 1/2\ MV^2$ in laboratory coordinates) collides with a free but initially stationary atomic electron (mass m_o, charge -e). If x is the impact parameter, then the differential scattering cross section per atomic electron, for an energy transfer between Q and Q = dQ, is (5)

$$d\sigma \equiv \Phi_o(Q)\, dQ = (2\pi z^2 e^4/m_o V^2 Q^2)dQ \text{ cm}^2/\text{electron}, \qquad (2\text{-}3)$$

where $\Phi_o(Q)$ characterizes the classical, non-relativistic collision theory. Then Eq. (2) becomes

$$(dT/ds)_{classical} = NZ \int_{Q_{min}}^{Q_{max}} (2\pi z^2 e^4/m_o Q V^2)dQ$$

$$= (2\pi z^2 e^4 NZ/m_o V^2) \ln Q_{max}/Q_{min} \quad \text{ergs/cm} \qquad (2\text{-}4)$$

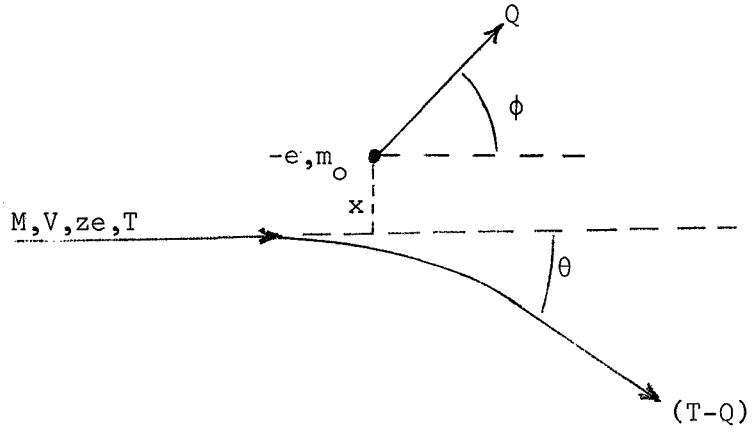

Figure 1

Schematic Representation of the Classical Coulomb Collision

Bohr (6) established values for Q_{max} and Q_{min} by relating the energy transfer, Q, to the impact parameter, x. The relationship between x and Q is given by

$$Q = 2z^2e^4/m_oV^2(x^2 + b^2/4) \tag{2-5}$$

where the collision diameter, b, is given by

$$b \equiv 2ze^2(M + m_o)/m_oMV^2 \tag{2-6}$$

Bohr then assumed that

(1) The maximum impact parameter $x = x_\nu$ is much greater than the collision radius. This is equivalent to permitting energy losses down to Q_ν, where $Q_\nu << 2TMm_o/(M + m_o)^2$. This minimum energy is much less than the work necessary to remove the electron from the atom.

(2) For impact parameters between x = 0 and x_ν, the atomic electrons behave as though they were completely unbound. For impact parameters greater than $x = x_\nu$, the electrons behave as though they were completely bound.

(3) Electrons which are displaced only slightly ($x > x_\nu$) return to the original configuration and absorb no energy.

Bohr further assumed that a bound electron, if excited by an incident particle but not ionized, would oscillate with a characteristic frequency, ν. In those collisions in which the effective time of collision, t, greatly exceeded $1/\nu$, there would be no energy transfer. Then if each atom has an individual characteristic frequency, ν_i, a geometrical mean value $\bar{\nu}$ is defined by

$$\bar{\nu}^Z = (\nu_1)(\nu_2)\ldots(\nu_Z). \tag{2-7}$$

Bohr's value for the maximum effective impact parameter, based on a detailed consideration of the energy transferred to the atomic electrons, could be expressed as

$$x_{\bar{\nu}} = 1.123\ V/2\pi\bar{\nu} \quad \text{cm}, \tag{2-8}$$

and Q_{min} would be expressed as

$$Q_{min} = 2z^2e^4/m_oV^2(1.123V/2\pi\bar{\nu})^2 \quad \text{ergs} \tag{2-9}$$

Since $x_{max} = 0$, the maximum energy transfer is

$$Q_{max} = 2m_o V^2 \, M^2/(M+m_o)^2 \qquad (2\text{-}10)$$

Now, Eq. (4) gives

$$(dT/ds)_{Bohr} = (4\pi z^2 e^4 NZ/m_o V^2) \, \ln 1.123 \, m_o MV^3/ \, 2\pi\bar{\nu} ze^2(M+m_o) \text{ ergs/cm.} \qquad (2\text{-}11)$$

In 1915, after he had derived his theory of quantized energy levels, Bohr (7) showed that Eq. (11) was valid only for those cases in which $V >> u$ (where u represents the orbital speed of the atomic electrons in their Bohr orbits) and in which $x_{max} = x_\nu$ was much greater than the radius of the Bohr orbit. For ionization in the K shell, this restriction implies

$$\beta \equiv V/c >> Z/137 \qquad (2\text{-}12)$$

On the other hand, $x_{max} = x_\nu$ corresponds to $Q_{min} = Q_\nu$, where Q_ν was much less than the ionization potential. Hence, this assumption led to a value for the energy loss which was too large for relativistic particles.

According to the theory of atomic structure, the minimum energy transfer in an atomic collision which produces an ionization event is the ionization potential of the electron. The mean value of this minimum energy of all the atomic electrons of the absorber is defined as the mean ionization potential

$$\ln I = \sum_n f_n \ln Q_{min} \qquad (2\text{-}13)$$

From the conservation laws for momentum and energy, it can be shown that the maximum energy transfer from an incident particle (rest mass M_o, relativistic kinetic energy $T = Mc^2 - M_o c^2$) to an initially stationary atomic electron (rest mass m_o) is

$$Q_{max} = T \left[\frac{1 + 2M_o c^2/T}{1 + (M_o m_o)^2 c^2/2m_o T} \right] \qquad (2\text{-}14)$$

If $M_o >> m_o$, then

$$Q_{max} = \frac{2m_o V^2}{1 - \beta^2} \left[\frac{1}{1 + (2m_o/M_o)(T/M_o c^2)} \right] \qquad (2\text{-}15)$$

If $M_o >> m_o$ and $M_o c^2 \geq T$, then (2-16)

$$Q_{max} = \frac{2m_o V^2}{1 - \beta^2}$$

Quantum Mechanical Theory

The theory of the stopping of swift charged particles was not improved further until the development of wave mechanics. Then the problem could be treated with partial wave analysis and the Born Approximation. (8)

In dealing with the problem quantum mechanically, the collisions are usually divided into two classes. Hard collisions are those in which the energy transfer varies from Q_{max} down to some arbitrary energy H. Soft collisions are those in which the energy transfer varies from H down to I, the mean ionization potential. This distinction is drawn because spin and exchange effects are important in the case of hard collisions, whereas they are negligible in soft collisions.

Bhabha (9) and others have calculated the cross section per atomic electron for primary particles of spin 0, 1/2, and 1, and the results have been summarized by Rossi and Greiser (10). For particles having spin 1/2, such as protons, the differential cross section for hard collisions is

$$d\sigma = \frac{2\pi z^2 e^4}{m_o V^2} \frac{dQ}{Q^2}\left[1 - \beta^2 \frac{Q}{Q_{max}} + \frac{1}{2}\left(\frac{Q}{T+M_o c^2}\right)^2\right] cm^2/electron. \quad (2-17)$$

Thus, the average energy loss is approximately given by

$$\frac{dT_H}{ds} = \frac{2\pi z^2 e^4}{m_o V^2} NZ\left(\ell n \frac{Q_{max}}{H} - \beta^2\right) \quad ergs/cm, \quad (2-18)$$

where H is arbitrary but must be large compared with the binding energy of the electron.

Bethe (11) derived detailed quantum-mechanical expressions for the energy lost in soft collisions by swift charged particles to bound electrons. He used the Born approximation to the method of partial wave analysis of soft collisions, which is valid if $2z/137\beta << 1$. For non-relativistic cases his method is equivalent to using a cross section proportional only to $\frac{dQ}{Q^2}$, and including all energy losses up to that of the head-on collision (12). Finally, the energy loss per unit path length becomes

$$\frac{dT_s}{ds} = \frac{4\pi z^2 e^4}{m_o V^2} NZ \ln \frac{2m_o V^2}{I} \qquad (2\text{-}19)$$

where I represents the geometric mean of all the ionization and excitation potentials of the absorbing atom. The fractional error in the first Born approximation is of the order u^2/V^2, where u is the Bohr-orbit velocity of the atomic electron. Hence, Eq. (19) is valid in the domain

$$\frac{u^2}{V^2} \simeq \frac{Z}{137\beta}^2 << 1 \qquad (2\text{-}20)$$

where u refers to the K electrons. A qualitative derivation of Eq. (19) is given by Williams (13).

Bethe (14) revised his original theory for relativistic particles with velocities, $V = \beta c$. The equation then is valid for soft collisions ($I < Q \leq H$) for incident particles of charge ze, provided $\beta >> Z/137$:

$$\left(\frac{dT_s}{ds}\right)_{Bethe} = \frac{2\pi z^2 e^4}{m_o V^2} NZ \left[\ln \frac{2m_o V^2 H}{I^2(1-\beta^2)} - \beta^2\right] \quad \text{ergs/cm.} \qquad (2\text{-}21)$$

Now combining the results for hard and soft collisions for the case of heavy particles with kinetic energy less than or equal to rest mass, one finds

$$\frac{dT}{ds} = \frac{4\pi z^2 e^4}{m_o V^2} NZ \left[\ln \frac{2m_o V^2}{I} - \ln(1-\beta^2) - \beta^2\right] \text{ergs/cm.} \qquad (2\text{-}22)$$

Shell Corrections

If the velocity of the incident particles is not large compared to the Bohr-orbit velocity of some of the atomic electrons (usually the case for heavy elements), Eq. (19) predicts too high a value for the energy loss. Bethe (15, 16) proposed the shell correction term to account for the ineffectiveness of various electrons. Walske (17, 18) has presented theoretical corrections for electrons in the K- and L- shells, and Bichsel (19) has extended the theory to include the M- shell. Sachs and Richardson (20) have proposed a theoretical correction to include all shells.

Using Walske's derivation, Bichsel (21) used the following procedure for obtaining the shell corrections. First, calculate the variable η_i, given by

$$\eta_i \equiv \frac{m_o c^2}{2Ry\ Z^2_{i\ eff}} \cdot \frac{\beta^2}{1-\beta^2} = \frac{18800}{Z^2_{i\ eff}} \cdot \frac{\beta^2}{1-\beta^2} \qquad (2\text{-}23)$$

where

$$Ry = 13.6 \text{ ev},$$

$$Z_{K\ eff} = Z - 0.3, \qquad (2\text{-}24)$$

$$Z_{L\ eff} = Z - 4.15,$$

$$Z_{M\ eff} \simeq Z - 14.$$

Then the shell corrections are given by

K-shell: For $\eta_K \geq 5$, $C_K = 1.22 \times 10^{-4}\ Z^2\ \frac{1-\beta^2}{\beta^2}$. (2-25)

For $5 > \eta_K \geq 0.5$, use Table 1 from Bichsel.

For $\eta_K > 0.5$, $C_K = (R_K \ln \eta_K + S_K - B_K)$, where

R_K and S_K are as in Table 2 and B_K in Table 3, also from Bichsel.

L-Shell: For $\eta_L \geq 3$, $C_L = P(Z)\eta_L^{-1} + 1.5\ \eta_L^{-2} - 4.0\ \eta_L^{-3} + 4.4\eta_L^{-4}$. (2-26)

For $3 > \eta_L \geq 0.7$, $C_L = \frac{Q(Z)}{\eta_L}$.

For $\eta_L < 0.7$ $C_L = R_L \ln \eta_L + S_L - B_L$, where $P(Z)$,

$Q(Z)$, R_L and S_L are in Table 2 and B_L is in Table 3.

M-shell: For $\eta_M > 0.3$, $C_M = 1.6 \times 10^{-4}(Z-14)^2 \cdot \frac{(1-\beta^2)}{\beta^2}$ (2-27)

Density Effect

Reduction in the emergy loss (and therefore the stopping power) of charged particles due to polarization of the medium must also be considered. Sternheimer (22) has summarized the theory and presented the results as the density effect, δ. The density effect can be written as

$$\delta = \Sigma_i\ f_i\ \ln[(\bar{\nu}_i^2 + \ell^2)/\bar{\nu}_i^2] - \ell^2(1-\beta^2) \quad , \qquad (2\text{-}28)$$

TABLE 1

Shell Correction C_K for $0.5 \leq \eta_K \leq 5$

$1/\eta_K$	Z = 11	Z = 32	Z = 100
0.20	0.450	0.460	0.465
0.25	0.537	.555	.560
0.30	.621	.635	.645
0.35	.694	.708	.720
0.40	.755	.776	.783
.45	.805	.831	.840
.50	.849	.878	.886
.55	.885	.916	.923
.60	.916	.947	.955
.65	.941	.973	.981
.70	.961	.993	1.003
.80	.982	1.019	1.033
.90	.983	1.029	1.043
1.00	.974	1.025	1.041
1.1	.958	1.013	1.031
1.2	.936	.991	1.013
1.3	.907	.966	.991
1.40	.873	.935	.964
1.55	.836	.903	.933
1.6	.796	.870	.899
1.7	.753	.833	.862
1.8	.711	.797	.824
1.9	.667	.757	.784
2.0	.619	.710	.745

TABLE 2

Data for Shell Corrections

K-shell			L-shell				
Z	$R_K(Z)$	$S_K(Z)$	Z	P(Z)	Q(Z)	$R_L(Z)$	$S_L(Z)$
11	1.813	2.463	20	1.50	1.70	10.037	28.145
18	1.722	2.404	30	1.88	2.06	7.912	24.450
32	1.646	2.346	45	1.99	2.17	6.745	21.906
65	1.581	2.287	100	2.00	2.18	6.034	20.015
100	1.553	2.257					

TABLE 3

Stopping Number Contribution of K- and L-shell Electrons

	B_K			R_L			
η_K or η_L	Z = 11	32	100	20	30	45	100
0.0	0.0	0.0	0.0	0	0	0	0
0.05	0.0	0.0	0.0	1.85	1.40	1.10	0.70
0.10	0.01	0.01	0.01	4.00	3.10	2.53	1.90
0.15	0.05	0.04	0.03	6.40	5.16	4.27	3.52
0.20	0.11	0.07	0.06	8.80	7.20	6.10	5.20
0.25	0.17	0.13	0.10	11.00	9.06	7.76	6.73
0.30	0.24	0.19	0.15	12.82	10.68	9.26	8.10
0.35	0.32	0.26	0.21	14.50	12.12	10.56	9.36
0.40	0.40	0.33	0.28	16.00	13.37	11.72	10.40
0.45	0.49	0.41	0.35	17.26	14.50	12.70	11.33
0.50	0.58	0.49	0.44	18.44	15.50	13.60	12.20
0.60	0.76	0.66	0.47	20.50	17.28	15.18	13.66
0.70	0.92	0.83	0.72	22.26	18.84	16.50	14.90
0.80	1.13	1.00	0.88	23.90	20.20	17.75	16.02
0.90	1.31	1.15	1.03	25.30	21.42	18.82	17.02

where f_i is the oscillator strength of the i^{th} transition (assuming that the dispersive properties of the absorber medium can be described as due to an arbitrary number of dispersion oscillators); ν_i is the frequency of the i^{th} transition; and $\not{\nu}$ is a frequency which is a solution to the equation

$$\frac{1}{\beta^2} - 1 = \sum_i \frac{f_i}{\nu_i^2 + \not{\nu}^2}$$

The density effect is an increaing function of the incident particle energy. In fact, below about 200 Mev, δ is negligible in comparison to the experimental errors.

Hence, the total average energy loss by ionization per unit path length per density of the stopping material is:

$$-\frac{dE}{\rho dx} = \frac{z^2 Z}{A} K(\beta) \left[f(\beta) - \ell n\, I - \frac{\sum_i C_i}{Z} - \frac{\delta}{2} \right] , \qquad (2\text{-}29)$$

where

$$K(\beta) = \frac{4\pi e^4 N_o}{m_o c^2 \beta^2} , \qquad (2\text{-}30)$$

$$f(\beta) = \left(\ell n \frac{2 m_o c^2 \beta^2}{1-\beta^2}\right) - \beta^2 , \qquad (2\text{-}31)$$

and

ρ = density of stopping material

z = charge number of incident particle

Z = atomic number of stopping material

A = atomic weight of stopping material

$\beta = \frac{v}{c}$, velocity of incident particle relative to velocity of light

C_i = shell correction of the i^{th} shell

δ = density correction at high energies

I = average excitation potential per electron of the stopping atom

e = electron charge

N_o = Avagadro's number

m_o = rest mass of electron.

Monte Carlo Theory

The discussion has thus far been limited in that only two types of interaction have been considered. First, if the closest distance between the incident particle and the atom is large compared to the size of the atom, then classical electromagnetic theory applies. Energy lost by the incident particles is transferred to the orbital electrons. As a result, the electrons may change orbits in an excitation process or leave the atom in an ionization process.

Secondly, if the incident particle passes the atom at a distance approximately the radius of the electronic orbits, a collision could result in which electron is pulled out of the atom. Due to the difference in mass between the proton and electron, at proton energies above 2 Mev no one of the discrete events induces more than a slight change in the energy or momentum of the incident proton. On the other hand, the electron can experience a large increase in energy, which is then dissipated in secondary electron-electron collisions.

There are certainly two other interactions which must be considered. The first is Rutherford scattering, which is significant whenever the proton enters the electric field of the nucleus. (The repelling force of the electric field should be corrected for the screening effect due to the electrons.) The angular distribution of outgoing protons for this interaction is highly forward-peaked, since the scattering amplitude is proportional to $\sin^{-4}(\theta/2)$.

The thickness of material through which 1/2 of the incident particles of energy E pass is defined as the median range, R (E). On the other hand, stopping power theory predicts the mean path length, P(E), given by (21)

$$P(E) = P(E_1) + \int_{E_1}^{E} \frac{1}{-dE/dx}\, dE \quad . \qquad (2\text{-}32)$$

The difference between range and mean path length is a result of multiple scattering. Due to the various Coulomb interaction, the incident particle travels a zigzag path through the absorber.

As Bichsel points out, the mean square fluctuation in the path length of the swift charged particle of energy E is given by

$$\sigma = \sqrt{(P^2)_{AV} - (P_{AV})^2} \qquad (2\text{-}33)$$

Although the straggling in mean path length can be represented by a Gaussian distribution, the asymmetry of multiple scattering processes leads to an asymmetric straggling distribution for range. Hence, the mean range is not identical to the median range.

Fourth, when the proton penetrates the nucleus, nuclear interactions occur. These reactions produce secondary particles of different types and energies which in turn travel through the absorber in all directions. Leimdorfer, Crawford, and coworkers (23) have incorporated all four types of interactions in a Monte Carlo transport theory for the stopping of swift charged particles. Linear transport theory deals with only the first two types, performing individual calculations for each discrete event. On the other hand, the Monte Carlo theory treats the problem as a continuous slowing-down process, using a multiple scattering model. For a particle slowing down between energies E_1 and E_2, multiple-scattering theory will give probable energy distribution and angular deviation for a given initial position, initial momentum, and final displacement for primary and secondary particles.

LIST OF REFERENCES

1. U. Fano, Annual Review of Nuclear Science (Annual Reviews, Inc., Palo Alto, California), 13, 1 (1963)
2. U. Fano and J. E. Turner, Nuclear Science Series Report #39, 49, (1964)
3. M.J. Berger and S.M. Seltzer, Nuclear Science Series Report #39,69 (1964)
4. Martin Leimdorfer, Monte Carlo Proton Transport Program. (NASA Grant NsG 708, Southern Methodist University, Dallas, 1965).
5. Robley D. Evans, The Atomic Nucleus (McGraw-Hill, New York, 1955), 1st ed., Appendix B.
6. N. Bohr, Phil. Mag. 25 10 (1913).
7. N. Bohr, Phil. Mag. 30, 581 (1915).
8. Robley D. Evans, The Atomic Nucleus (McGraw-Hill, New York, 1955), 1st ed., Appendix C.
9. H. J. Bhabha, Proc. Roy. Soc. (London) A164, 257 (1938).
10. B. Rossi and K. Greisen, Revs. Mod. Phys. 13, 240 (1941).
11. H. A. Bethe, Ann. Physik 5, 325 (1930).
12. E. J. Williams, Proc. Roy. Soc. (London) A135, 108 (1932).
13. E. J. Williams, Revs. Mod. Phys. 17, 217 (1945).
14. H. A. Bethe, Z. Physik 76, 293 (1932).
15. M. S. Livingston and H. A. Bethe, Revs. Mod. Phys. 9, 245 (1937).
16. H. A. Bethe and J. Ashkin in E. Segre (ed.), Experimental Nuclear Physics (John Wiley and Sons, New York, 1953), Vol. 1, p. 166.
17. M. C. Walske, Phys. Rev. 88, 1283 (1952).
18. M. C. Walske, Phys. Rev. 101, 940 (1956).
19. H. Bichsel, "Higher Shell Corrections in Stopping Power," Technical Report No. 3, 1961.
20. D. C. Sachs and J. R. Richardson, Phys. Rev. 83, 834 (1951); 89, 1163 (1953); 94, 79 (1954).
21. H. Bichsel, "Passage of Charged Particles through Matter," Technical Report No. 2, 1961.
22. R.M. Sternheimer, Phys.Rev.88 (1952); 93, 351 (1954); 91, 256 (1953).
23. Martin Leimdorfer, unpublished research and private communications.

CHAPTER 3

THEORETICAL BACKGROUND FOR PROTOS 3

by Claes Johansson and Martin Leimdorfer

INTRODUCTION

The analysis of the transport of charged particles in matter is a vital problem in many branches of radiation science such as radiation biology, cosmic radiation physics, space radiation shielding, and medical radiology. It has attracted the interest of many prominent theoretical physicists, notably Bethe, Bohr, Fermi, and Landau.

The migration of protons (or charged particles in general) in matter is determined by a multitude of interaction processes. We may distinguish between the following principal types.

1) If the distance of closest approach between the moving proton and the atom is large compared to the dimensions of the atom, we may apply the classical picture of a moving point charge creating a variable electromagnetic field which dissipates energy in the outer electronic shells of the atom. As a result, one or more electrons may be either transferred from one orbit to another (excitation) or totally removed from the atom (ionization).

2) If the distance of closest approach is of the order of the outer electronic orbits, the proton may interact with a single electron which is then thrown out of the atom (a "knock-on" process) and the remaining electrons rearrange themselves to the configuration of highest stability.

The proton energies to be considered are always above 2 MeV. This means that the energy loss due to excitation will be comparatively small. The energy taken from the proton when an electron is ejected from the atom is also small due to the great difference in weight between the two particles. By the same arguments we see that the direction and magnitude of the proton's momentum will also be changed by very small values at each discrete event. For all practical purposes the directional change may in fact be neglected altogether.

3) When the distance of closest approach is small enough to admit the proton into the interior of the atom, the main mode of interaction is the repellant effect of the electric field of the nucleus (Rutherford scattering) which has to be corrected for the screening of the electric field caused by the electrons. The momentum transfer in this type of interaction is also small and therefore the angular distribution of outgoing protons is highly forward-peaked.

4) If, finally, the proton reaches within the very short range of the nuclear forces, a nuclear interaction may occur. We distinguish

between elastic and non-elastic collisions. In the first type the proton will only be deflected by the nuclear potential, and the energy loss will be equal to the elastic recoil of the nucleus. The term non-elastic collision covers all the different processes in which the proton penetrates into the nucleus and other particles are ejected.

To avoid the complicated and cumbersome treatment of each discrete collision, a continuous slowing-down theory has been established, the multiple-scattering model. The migration process may be described by the following example: Consider a particle slowing down between the energies E_1 and E_2 starting at a fixed point and in a given direction. Multiple-scattering theory will, in principle, give us the probability distribution of possible spatial points at which the energy E_2 is reached by the particle. Alternatively, we may ask for the distribution in energy and deviation angle when a particle travels a certain distance in space.

ENERGY LOSS

We have decided to apply a Monte Carlo scheme based on a picture where the protons slow down in energy step-wize between a set of predetermined energy points. This procedure has many advantages in the practical computation work. We select a set of energies (E_i) in the energy region from the source energy to the cut-off energy E_n, 2 MeV $< E_n = \min(E_i)$, and sample the spatial displacements from the appropriate distributions for each energy drop between two successive energy points. The lower energy limit of 2 MeV is chosen to represent the energy at which the residual range of the particle is negligible, that is, where the proton history may be effectively terminated. (This is convenient also for the reason that multiple-scattering theory gradually ceases to work below this limit). The points in the predetermined set of energies are selected uniformly in a) the logarithm of the energy, b) in a linear relationship or c) supplied as data. This implies that $E_{i+1} = k.E_i$ where k is a constant factor and E_i and $E_{(i+1)}$ are two of the successive energy stopping points. We calculate the factor k from the relation $k = (E_o/E_n)^{1/n}$ where E_o is the source energy (in MeV) and n is the number of portions into which we divide the slowing-down process.

There are several advantages in the choice of such a logarithmic energy mesh. One of the most important ones is that the mean deviation angle is practically constant if, as here, the energy is decreased by a constant factor. This improves the computation efficiency. We shall come back to this aspect below.

ANGULAR DEFLECTION

When considering the spatial displacements suffered by the proton when traveling down in energy between two successive energy points, we shall treat separately the deviation of the particle from its initial direction. Moliere has developed a theory (2) for calculating the statistical distribution of deflection angles in the multiple-scattering

model. Moliere's initial work has been improved and extended by Bethe (3) and Fano (4), and we shall only indicate the line of reasoning and present the results.

The Moliere method produces a distribution of angular deviations that are coupled to the slowing down of the migrating particle between two given energies. The result is an average over all the possible means of loosing the given amount of energy by a great number of electromagnetic interactions with atoms of the medium. The angular distribution converges to the single-scattering (Rutherford) distribution at large angles. Bethe (3) has analyzed the convergence mechanism. He shows that the Moliere distribution converges to the small-angle Rutherford scattering approximation

$$X(\theta)d\theta \simeq d\theta/\theta^3 \qquad (3\text{-}1)$$

rather than the correct formula

$$X(\theta)d\theta \simeq \sin\theta\, d\theta/\sin^4(\theta/2) \qquad (3\text{-}2)$$

but points out that this discrepancy is compensated almost exactly by other approximations (cf. (3), page 1263). In all cases the distribution is modified at small angles by the introduction of a "screening angle" to remove the singularity at $\theta = 2n\pi$. It may be remarked that the Moliere distribution does not include a spin-dependent part corresponding to the Mott single-scattering distribution

$$X(\theta)d\theta \simeq (1 - \beta^2\sin^2\frac{\theta}{2})\sin\theta\, d\theta/\sin^4(\theta/2) \qquad (3\text{-}3)$$

(for spin 1/2, cf. (10), page 64)

This implies that the Moliere distribution may fail at high energies where the relativistic correction becomes important. It should be pointed out, however, that in general $\theta << 1$ and hence the discrepancy is not so serious.

Moliere introduces a "reduced scattering angle" θ , related to the deflection angle ω by the relation $\theta = \omega/X_c\sqrt{B}$. The Moliere distribution has the form

$$A(\omega)d\omega = \theta d\theta\, \{2\exp(-\theta^2) + f^1(\theta)/B + f^2(\theta)/B^2 + \ldots\ldots \qquad (3\text{-}4)$$

where $f^{(i)}(\theta)$ are numerical functions tabulated by Bethe (3). The above truncation of the expansion is sufficient to determine the distribution function to better than 1 percent at any angle (cf. (3),

page 1260). The functions X_c and B are evaluated in the following way:

First set

$$X_c'^2 = 4\pi N Z^2 e^4 / p^2 v^2 . (4\pi\varepsilon_o)^2 \qquad \text{(in MKSA units)} \qquad (3\text{-}5)$$

p and v are the relativistic momentum and velocity of the proton, respectively. N is the number of atoms per unit volume, Z the atomic number of the scatterer, and e the electron charge. The product p^2v^2 may be transcribed to read

$$\left[E + mc^2 - m^2c^4/(E + mc^2)\right]^2 \qquad (3\text{-}6)$$

where E is the kinetic energy of the particle. X_c is then obtained by integrating

$$X_c^2 = \int_{E_{i+1}}^{E_i} X_c'^2(E') \cdot \left|\frac{dE'}{ds}\right|^{-1} dE'. \qquad (3\text{-}7)$$

dE'/ds may be computed from the Bethe-Bloch formula Equation 2-29, as required for the calculation, or obtained from tables of dE/ds versus energy stored in the computer for the specific material under consideration.

The variable B is calculated from the following relations

$$X_a^2 = 2.01 \cdot 10^{-11} \cdot Z^{2/3}\left[1.13 + 3.76\ (Z/137\beta)^2\right] \qquad (3\text{-}8)$$

$$\text{where } \beta = \frac{v}{c} = \left[1 - m^2c^4/(E + mc^2)^2\right]^{\frac{1}{2}} \qquad (3\text{-}9)$$

$$\log X_a^2 = \frac{1}{X_c^2}\int_{E_{i+1}}^{E_i} X_c'(E') \log X_a^2(E') \left|\frac{dE'}{ds}\right|^{-1} dE' \qquad (3\text{-}10)$$

and we obtain B from the transcendental equation

$$B - \log B = \log \frac{X_c^2}{1.167(X_a^2)} + \frac{1}{Z}\left\{\log\left[11.30\ Z^{-4/3} \cdot \frac{\beta^2}{1-\beta^2}\right] - c_F - \frac{1}{2}\beta^2\right\} \qquad (3\text{-}11)$$

which includes Fano's correction to make Moliere's formula valid for protons (1). The constant c_F was taken from an estimate by Fano, reproduced in ref. (1). A graph showing the variation of c_F with Z is presented in fig. 1.

In the computation a table of the values of X_c and B at all E_i is prepared before the start of the actual Monte Carlo procedure. The final selection of an angle θ from the Moliere distribution could now be made in the straightforward way by solving the equation

$$R(0,1) = \int_0^{\theta} \theta' d\theta' \{2\exp(-\theta'^2) + f^1(\theta')/B + f^2(\theta')/B^2 + \ldots\ldots\} = g(\theta) \qquad (3\text{-}12)$$

where R(0,1) is a random number, equi-distributed on the unit interval. This procedure is extremely laborious, and we chose an alternative technique instead. First, we set up a table of θ-values corresponding to the $g(\theta)$ values 1/80, 3/80, 5/80,....79/80, neglecting the $f^{(1)}$ and $f^{(2)}$ terms which are, in effect, relatively small corrections. This table is readily constructed by analytical integration. The $f^{(i)}(\theta)$ functions are then integrated numerically between 0 and the θ-values obtained in the previous operation. When an angle is selected, a table of the full integral (with the proper value of B inserted) is made up which contains the θ-values obtained from the simplified distribution but the $g(\theta)$ values corrected by the two additional terms. It is then easy to obtain an angle by using a sampled random number and a simple table look-up and interpolation technique. All the integration work and the solution of B is performed for each energy step before the start of the Monte Carlo procedure. The calculations that remain to be made to obtain the angle in the actual Monte Carlo cycle are then very rapid.

DISTANCE TRAVELED BETWEEN REFERENCE ENERGIES

The distance s_i that a proton travels in space simultaneously as it is slowed down between two successive energy stops, E_i and E_{i+1}, is, on the average, equal to

$$\langle s_i \rangle = \int_{E_{i+1}}^{E_i} dE / |dE/ds| \qquad (3\text{-}13)$$

Because of the inherent fluctuations in the multiple scattering process, the real distances traveled are distributed according to some statistical distribution around this mean. This effect is called straggling. Sternheimer (6) has studied the phenomenon, and using his results, we obtain the following relation for the variance of the distribution:

$$\langle \Delta s^2 \rangle_i = \left[\langle s^2 \rangle - \langle s \rangle^2\right]_i = \frac{4\pi e^4 N}{(4\pi\varepsilon_o)^2} \int_{E_{i+1}}^{E_i} \frac{(1 - \frac{1}{2}\beta^2) K dE}{(1-\beta^2)\left[1 + \frac{2m_e}{m_p} \cdot \sqrt{1-\beta^2}\right]} \left|\frac{dE}{ds}\right|^3 \qquad (3\text{-}14)$$

where m_e/m_p is the electron to proton mass ratio and K is a factor that takes account of the effects of binding of the atomic electrons which is important only for low proton energies (for Al, K=1.33 at 2 MeV and K=1.04 at 100 MeV). The expression for K has been given by Bethe (7). Sternheimer in (6) presents the total broadness of the distribution of distances traveled by protons until they reach 2 MeV (by setting the lower energy (E_{i+1}) of the above integral equal to 2 MeV). The actual pathlength is sampled from a Gaussian distribution, with mean $\langle s_i \rangle$ and variance $\langle \Delta s^2 \rangle_i$; $\langle s_i \rangle$ is obtained according to its definition, using values of the stopping power dE/ds from Chapter 7.

SPATIAL DISPLACEMENT

We have now assessed the length of the path that the proton travels between two energy stops and the deviation in angle at the end of a step from the direction at the start of the step. The deflection in azimuthal angle can be safely taken as random as many discrete collisions are involved, and no polarization has to be considered. One assumption has to be made concerning the projected length of a path on the initial direction of the paticle at the start of the specific path ($\Delta\zeta$) . We follow Berger (1) and set

$$\Delta\zeta = \langle s \rangle \frac{1 + \cos \omega}{2} \qquad (3\text{-}15)$$

which can be proved to be correct on the average and also in the limit of very small values of ω , as is always the case in our problems. The displacements along two mutually perpendicular axes in a plane normal to $\Delta\zeta$ are taken as (1)

$$\Delta\zeta = \frac{1}{2}\langle s \rangle (\sin \omega \cos \Delta\phi + k_x (\omega^2/\varepsilon)^{\frac{1}{2}}) \qquad (3\text{-}16)$$

$$\Delta\eta = \frac{1}{2}\langle s \rangle (\sin \omega \sin \Delta\phi + k_y (\omega^2/\sigma)^{\frac{1}{2}}) \qquad (3\text{-}17)$$

where $\Delta\phi$ is a random asimuthal angle and k_x and k_y are two uncorrelated numbers picked from a normal distribution (Gaussian) with mean zero and variance unity. The formulae were derived by Rossi (10).

CALCULATION GEOMETRY

We have outlined the treatment of the energy and space displacements of a proton in the slowing-down procedure. It is now necessary to specify a geometrical system of coordinates in which the particles are to move. We have chosen a Cartesian (x,y,z) system with the z-axis along the direction of motion of the protons at the beginning of the

slowing-down process. The problem geometry considered in the present version of the related computer program (see below) is a solid rod with either square or circular cross-section. The source protons are entered in the direction of the axis of the cylinder, uniformly over a circular surface of prescribed radius centered on the axis.

The relations between the displacements in the $(\zeta, \eta, \zeta,)$ and the (x,y,z) system of coordinates are obtained from the equations

$$\Delta x = -\cos\theta_i \cos\phi_i \Delta\zeta + \sin\phi_i \Delta\eta + \sin\theta_i \cos\phi_i \Delta\zeta \quad (3\text{-}18)$$

$$\Delta y = -\cos\theta_i \sin\phi_i \Delta\zeta - \cos\phi_i \Delta\eta + \sin\theta_i \sin\phi_i \Delta\zeta \quad (3\text{-}19)$$

$$\Delta z = \sin\phi_i \Delta\zeta + \cos\theta_i \Delta\zeta \quad (3\text{-}20)$$

Here, θ_i and ϕ_i are the angles of the particle path with the z-axis and of the projection of the path on the x-y plane at the beginning of the i:th step, respectively. The corresponding angles at the beginning of the next step, θ_{i+1} and ϕ_{i+1}, are obtained from the relations

$$\cos\theta_{i+1} = \cos\theta_i \cos\omega + \sin\theta_i \sin\omega \cos\Delta\phi \quad (3\text{-}21)$$

$$\sin(\phi_{i+1}-\phi_i) = \frac{\sin\omega \sin\Delta\phi}{\sin\theta_{i+1}} \quad (3\text{-}22)$$

$$\cos(\phi_{i+1}-\phi_i) = (\cos\omega - \cos\theta_i \cos\theta_{i+1})/\sin\theta_i \sin\theta_{i+1} \quad (3\text{-}23)$$

extracted from ref. (1).

COMPUTER PROGRAM

A computer program (PROTOS 3), based on the above outline, has been coded in FORTRAN language for the IBM-360/44 computer to provide energy, direction, and space distributions of escaping protons. The number of proton histories required to obtain well-converged results, of course, varies with the problem, but it may be said that in general at least one thousand histories have to be run.

NUCLEAR REACTIONS

The insertion of the possibility of nuclear interactions was carried out in PROTOS III. As some of the charge particles that may emerge from the nucleus are different from protons, our treatment had to be modified. This did not necessitate any major alterations. The transport of the

uncharged particles calls for a different treatment, but well established procedures can be applied for that case.

A NOTE ON THE MEAN IONIZATION POTENTIAL

The mean energy loss by ionization, dE/dx, which is a crucial quantity in the model which we have applied depends on the mean ionization potential I, of the atom or molecule. A table of recommended values of stopping power for various elements and compounds is included as a separate chapter.

LIST OF REFERENCES

1. M. J. Berger: In "Methods in Computational Physics," vol. I. Ed. by B. Alder, et al. (1963).
2. G. Moliere: Z. Naturforsch. 3a (1948) 78.
3. H. A. Bethe: Phys. Rev. 89 (1953) 1256.
4. U. Fano: Phys. Rev. 93 (1954) 117.
5. H. A. Bethe: Handbuch der Physik. 24.1 (1933) 518.
6. R. M. Sternheimer: Phys. Rev. 117 (1960) 485.
7. M. S. Livingston and H. A. Bethe: Revs. Mod. Phys. 9 (1937) 261.
8. R. M. Sternheimer: Phys. Rev. 115 (1959) 137 with an erratum in Phys. Rev. 124 (1961) 2051.
9. H. W. Lewis: Phys. Rev. 85 (1952) 20.
10. B. Rossi: "High Energy Particles," Prentice Hall (1952).
11. H. W. Bertini: ORNL-3383 (1963).
12. U. Fano: Ann. Rev. Nucl. Sc. 13 (1963) 1.
13. R. M. Sternheimer: Phys. Rev. 118 (1960) 1045.

CHAPTER 4

A PROGRAM SYSTEM FOR SIMULATING THE TRANSPORT OF NEUTRONS AND PROTONS AT THE ENERGIES BELOW 400 MEV

by Martin Leimdorfer and George Crawford

INTRODUCTION

The PROPER 3B system is a series of computer codes for treating problems of nucleon transport under the influence of nuclear as well as Coulomb forces. The existing version permits a geometry of a homogenous rectangular rod of square cross section. The source particles may be composed of an arbitrary mixture of protons and neutrons. The energy, space, and directional distribution of incident particles may be set arbitrarily or chosen from a few built-in generating functions. The energy range of the present version is from 0 to 400 MeV. The original versions of the components of the code system have been initially developed at several installations, viz. Atomic Weapons Research Establishment (AWRE), Aldermaston, England, Atomic Energy Establishment, (AEEW), Winfrith, England (the neutron cross section tapes at energies below 14 MeV), Oak Ridge National Laboratory (ORNL), Oak Ridge, Tenn. (nuclear interaction data at energies 25 - 400 MeV), Research Institute of National Defense (FOA), Stockholm, Sweden (particle transport and cross section processing programs). The complicated task of modifying and linking these codes (and in some cases modernizing them considerably) was undertaken by Southern Methodist University (SMU), Dallas, Texas.

LAY-OUT OF THE PROPER 3B CODE SYSTEM

Figures 4-1 and 4-2 show flow charts which are meant to display, in a concise form, the logical sequence of appearance of the components (1 through 13) of the code system. Components 1 through 7 (see Figure 4-1) are the portion of the system used to compute the data, underlying the handling of nuclear interactions in the high-energy part of the calculation (400 MeV - 25 MeV). The basic development of this part was performed at Oak Ridge National Laboratory.

1. Nuclear Evaporation and Cascade Calculations:

   Full descriptions of the techniques used in the boxes labeled 1a and 1b of Figure 4-1, are given by Bertini (1) and Leimdorfer and Barish (2), respectively.

2. CASEVA

   The CASEVA program as written by A. Henriksson and A. Ottosson (3) is used to edit these data in a form suitable for application to the PROPER 3B system. The CASEVA code produces a magnetic tape, 3, filled with nuclear interaction data for the elements C, O, Al, Cr, Cu, Ru, Ce,

W, Pb, and U-238. If more elements are to be added, they must be listed in the proper sequence of increasing value of Z. These data are used to interpolate data for other elements with atomic masses in the range from 12 through 238, using the method of Leimdorfer and Barish (2). In the present version of the PROPER system, elements in the range from 2 through 11 cannot be handled. The data for hydrogen were taken from the compilation of Bertini (4).

3. High energy nuclear data tape, 3, contains all the information produced in the components 1 and 2 of the PROPER 3B program. This MTAPE (binary) is the tape written by the CASEVA program.

4. INTPOL

The INTPOL program, 4, originally written by A. Ottosson and modified by E. Helwig, performs the interpolation to create an Intermediate Data Tape from MTAPE 3 to be used as input to the REDIG program. INTPOL can perform three kinds of functions:

a. Create data or an element not present on MTAPE 3 by linear interpolation between two elements that are on MTAPE 3.

b. Copy data from MTAPE 3 to an Intermediate Data Tape. To use the copy feature, set Z0 = Z1 = ZNEW and AA = A0 ≠ A1.

c. Skip to the end of existing intermediate data tape in order to add more data to it. To skip, set Z0 = the identification of the element on the intermediate data tape beyond which one wishes to skip. Set A0 = a negative number. Ignore all other items in Card B.

INTPOL Input uses two cards having the following form:

```
                  a   b   c   d   e
Card A:  Format (I5, I5, I5, I5, I5)
```

a. NUMBER: The number of elements for which data are requested in the run.
b. KTAPE: The logical number assigned to tape 1.
c. LTAPE: The logical number assigned to tape 2.
d. MTAPE: The logical number assigned to the input tape.
e. NTAPE: The logical number assigned to the output tape.

Card B: (to be repeated for each element for which data should be produced in the run)

```
                  a      b     c      d     e      f     g
        Format (A4, F10.0, A4, F10.0, A4, F10.0, A4)
```

a. Z0: The atomic number of the lighter element of those used in the input.

b. AO: The atomic weight of the element under a.
c. Z1: The atomic number of the heavier element of those used in the input.
d. A1: The atomic Weight of the element under c.
e. ZNEW: The atomic number of the new element. (ZO < ZNEW < Z1)
f. AA: The atomic weight of the element under e. (AO < AA < A1)
g. ELMENT: Alphanumeric name of the new element.

This card may be repeated as many times as desired. An End-Block card informs INTPOL that there is no more data.

Input Tape
MTAPE (binary) is the tape written by the CASEVA program 2.
INTPOL Output Tape: NTAPE (binary)

MTAPE and NTAPE contain two records for each element. The first record contains:

MTAPE	NTAPE	
Z	ZNEW :	The atomic number of the element requested.

The second record contains:

MTAPE	NTAPE	
ATOMV	AA:	The atomic weight.
ELMENT	ELMENT:	The name of the element requested.
BTAB	BTABNY:	The energy of evaporation particles in MeV.
ATAB	ATABNY:	Cosine for the scattering angle.
FACT	FACTNY:	E/E_o in sampling vector.

MTAPE	NTAPE	
NSPK	NSPKNY:	The number of secondary cascade particles per reaction
NSPE	NSPENY:	The number of secondary evaporation particles per reaction
SIGMA	SIGMNY:	Cross sections (in barns).

Dimensions of Arrays:

BTAB	9 21 2 2 (JE, I, IN, UT)
ATAB	9 11 2 2 (JE, I, IN, UT)
FACT	9 11 41 2 2 (JE, L, I, IN, UT)
NSPK	9 2 2 (JE, IN, UT)

	9	2	2	
NSPE	(JE,	IN,	UT)	
	9	2		
SIGMA	(JE,	IN)		

JE: Number of argument energy points (9).

I: Number of values per IN - UT-combination and energy group.

L: Number of cosine values per IN - UT-combination and energy group.

IN: The incoming particle is a proton if IN = 1, if IN = 2 the incoming particle is a neutron.

UT: The secondary particle is a proton if UT = 1, if UT = 2 the secondary particle is a neutron.

Subroutine RESTO sets a desired value (a) in the vector A with length b. RESTO is called by the statement CALL RESTO (A, a., b)

INTPOL prints pairs of numbers while reading the data tape. The first number is the Z of the element just read, the second number is the Z of the element it is searching the tape to find.

INTPOL prints the symbols, INTPOL TERMINATED NORMALLY, when the program has completed a successful run.

5. BINOUT

The BINOUT program, 5, written by A. Ottosson, edits data tapes in a decimal form suitable for checking. It is a FORTRAN IV program that produces edited decimal listings of the tapes written by the programs CASEVA, 2, INTPOL, 4, and REDIG, 6.

The input card contains the following information.

	a	b	c	d	e	f
Format	(I10,	I10,	I10,	I10,	I10,	I10)

a. Number: Number of elements or mixtures for which data are to be listed.
b. IBTAB: Number of BTAB values (presently always equal to 21).
c. IATAB: Number of ATAB values (presently always equal to 11).
d. IFACT: Number of FACT values (presently always equal to 41).
e. MTAPE: Logical number assigned to input tape for this program.
f. NAME: An integer which is equal to 0 when CASEVA or INTPOL tapes are handled.

The print-out provided by BINOUT is arranged as follows:

		a	b	c
A.	Heading: Format	(A4,	F10.5,	A4)

a. Z: Atomic number or other identification number.
b. ATOMV: Atomic weight or density.
c. ELEMNT: Name given the element or compound.

B. BTAB: Format (1P 4E20.7)
Table of equiprobable energies of evaporation particles arranged in order of increasing values. Four columns are given on each printed page.
First column: proton in, proton out
Second column: neutron in, proton out
Third column: proton in, neutron out
Fourth column: neutron in, neutron out
Every argument energy point corresponds to 21 lines.

C. ATAB: Format (1P 4E20.7)
Table of cosines for the scattering angles arranged as described under B.
Every argument energy point corresponds to 11 lines.

D. FACT: Format (1P 4E20.7)
Table of equiprobable values of E/E_0, arranged in order of increasing scattering angle and of increasing energy. Arrangement of columns according to B. Every group of constant scattering angle consists of 41 lines and every group of constant energy consists of 451 lines.

E. NSPK: Format (1P 4E20.7)
Table of the number of secondary cascade particles arranged in order of increasing energy. Arrangement of columns according to B. Every argument energy point corresponds to one line.

F. NSPE: Format (1P 4E20.7)
Table of the number of secondary evaporation particles arranged as described under E.

G. SIGMA: Format (1P 2E20.7)
Table of cross sections (in barns) arranged in order of increasing energy. Two columns are given.
First column: incoming particle = proton
Second column: incoming particle = neutron
Every argument energy point corresponds to one line.

When listings of tapes written by programme REDIG, SIGMA is changed to LAMBLA (H) and PH is included (I).

H. LAMBLA: Format (1P 2E20.7)
Table of mean free paths (centimeters) arranged as described under G.

I. PH: Format (1P 2E20.7)
Table of probabilities for interacting with hydrogen arranged as described under G.

6. REDIG

The REDIG, program produces the final data tape, 7, to be used in the particle transport simulation. The program was written by A. Ottosson and modified by E. Helwig. The data for pertinent elements, which is produced by either the CASEVA 2 or INTPOL 4 program is used as input. The program then computes data for a mixture or compound, with given composition and density, consisting of from one to five elements. The program can be readily extended to increase the number of elements to be used in a compound or mixture.

Cross sections (in barns) for proton-proton and neutron-proton interactions at nine argument energies (25, 50, 100, ,50, 200, 250, 300, 350, 400 MeV) in order of increasing energy. The first set of nine numbers are p-p data and the second set of nine numbers are n-p data. The following values are in a data statement (taken from ref. 4 of the main text): 0.14; 0.06; 0.028; 0.025; 0.024; 0.024; 0.024; 0.024; 0.024; 0.4; 0.18; 0.073; 0.052; 0.044; 0.038; 0.035; 0.034; 0.033.

Input (compare input to INTPOL program):

		a	b	c	d
Card A:	Format	(I5,	I5,	I5,	I5)

a. Number: The number of compounds or mixtures for which data are requested in the run.
b. KTAPE: The logical number assigned to tape 1.
c. LTAPE: " " " " " " 2.
d. NTAPE: " " " " " output tape.

		a	b	c	d	e	f	g	h	i	j
Card B:	Format	(A4,	F10.0,	A4,	F10.0,	A4,	F10.0,	A4,	F10.0,	A4,	F10.0)

a. ZO: The atomic number of element 1.
b. NA: Number of nuclei per unit volume of element 1 (in nuclei per $cm^3 \times 10^{-24}$).

c. Z1: Same as a. but for element 2.
d. NB: Same as b.

e. Z2: Same as a. but for element 3.
f. NC: Same as b.

g. Z3: Same as a. but for element 4.
h. ND: Same as b.

i. Z4: Same as a. but for element 5 (if hydrogen is present,
j. NE: Same as b. this element is hydrogen).

Card B1: Format (F10.0, F10.0, I5, A4, A4)
a b c d e

a. NH: Number of hydrogen nuclei per unit volume (in nuclei/cm^3 x 10^{-24}). If no hydrogen, NH = 0 (or blank). If NH ≠ 0, NH must be set equal to NE of card B.
b. DENSIT: Density of medium (grams per cm^3); only for identification purposes.
c. NR: Number of elements in the compound or mixture under consideration, excluding hydrogen. (E.g. for NaOH, NR = 2.)
d. IDENT: Identification number of the new material.
e. ELEMENT: Name or formula of the new material.

Card B must be given for each material to be considered in one run. It may be repeated for as many materials as desired. Considerable running time can be saved by putting the elements used to define each new material (Z1, Z2, ...) in increasing order of Z on Card B.

The Input Tape is the MTAPE (binary) obtained as output from CASEVA 2 or INTPOL 4 programs. The Output Tape, NTAPE 2, (binary), consists of two records for each material. The first one contains the identification number, IDENT, of the material.
The second record contains,

DENSIT: The density of the material (as given in input).
ELMENT: The name or formula of the material (as given in input).
BTABNY: Equiprobable energies (in MeV) of evaporation particles.
ATABNY: Equiprobable cosines of cascade particle deviation angles.
FACT: Equiprobable values of normalized energy (E/E_o) for cascade particles.
NSPKNY: Number of cascade particles per collision.
NSPENY: Number of evaporation particles per collision.
LAMBLA: Mean-free-paths (in centimeters).
PH: Probabilities for hydrogen interaction.

Dimensions of Arrays:

BTABNY	9 21 2 2 (JE, I, IN, UT)
ATABNY	9 11 2 2 (JE, I, IN, UT)
FACT	9 11 41 2 2 (JE, I, L, IN, UT)
NSPKNY	9 2 2 (JE, IN, UT)
NSPENY	9 2 2 (JE, IN, UT)

	9	2
LAMBLA	(JE,	IN)
	9	2
PH	(JE,	IN)

JE: Number of energy groups.
I: Number of values per IN - UT-combination and argument energy.
L: Number of cosine values per IN - UT-combination and argument energy.
IN The incoming particle is a proton if IN = 1, if IN = 2 the incoming particle is a neutron.
UT: The secondary particle is a proton if UT = 1, if UT = 2 the secondary particle is a neutron.

The subroutine RESTO is called by the statement CALL RESTO (A, a., b). It sets a desired value (a) in the vector A with length b. When the program is complete, a printout, REDIG TERMINATED NORMALLY, is typed out.

7. Final High-Energy Nuclear Data Tape:
The output tape from REDIG, NTAPE 7, contains the data in the form necessary for input into the PROTOS III Monte Carlo program 9 The PROPER 3B code package contains magnetic tapes for the elements C, Al, Si, Cu, Fe, and Pb with naturally occurring densities. In addition, tapes are provided for the mixtures given in Table 4-1.

Table 4-1

List of element mixtures for which high-energy nuclear data are provided in the PROPER 3B code package

Name	Chem. symbol	Density (grams/cc)	No. of atoms per cc $\cdot 10^{-24}$ H	C	N	O
Water	H_2O	1.0	0.067	0	0	0.0335
Polythene I	CH_2	0.95	0.08174	0.04087	0	0
"	"	0.915	0.07873	0.03936	0	0
Nylon	$C_{12}\ H_{22}\ O_2\ N_2$	1.1399	0.06683	0.02083	0.06074	0.006076
Tissue	"$C_{27}\ H_{21}\ O\ N$"	1.0999	0.0371	0.04769	0.00176	0.00177
Lucite	$C_5\ H_8\ O_2$	1.1892	0.0573	0.03581	0	0.01433

Any other elements (having masses between the range of 12 and 238) or mixtures using hydrogen and the above elements can be used in the PROTOSIII program. Data for the NTAPE 7 for these would be created by following the above instructions.

8. Source

The SOURCE program, written by Claes Johansson, uses the distribution of positions, energies, and directions of entry for both neutrons and protons as supplied by the user. In the program PROTOS 3 a dummy subroutine SOURCE(NT) is called as one way of generating source particles for the program. However, the user of PROTOS can supply his own program SOURCE(NT) and this is written to clarify the format. The argument of the subroutine NT means the total number of source particles and is normally read by PROTOS and supplied to source, but it can be changed by source.

The source routine gives the particles as NT records, each containing 12 data in the following order:

MS	index of particle energy in energy scale, if particle energy is EO (see below) then MS = 1.
X	
Y	Coordinates, The PROTOS body is standing
Z	on X, Y plane with the Z-axis as a center.
SLAT = 1	at present, will become particle weight.
CTH	Cos(θ) polar angle (with Z-axis)
STH	Sin(θ)
CFI	Cos(α) azimuthal angle (in X-Y plane)
SFI	Sin(α)
NP	= 1 for a proton, = 2 for a neutron.
E	energy (EK(MS) $\geq$ E > EK(MS + 1) defines MS
NSOU	Number of source particle (1, 2...NT)

The information that might be needed to write SOURCE is in COMMON/MAIN/ which for this purpose looks like this

COMMON/MAIN/EK(100), DUMMY 1(510), M, Ru, Du, NT, IG, DUMMY2(5), EO

EK	main energy scale down from EO = EK(1) to EK(M)
RU	radius or half side of PROTOS body
DU	length of body 0 < Z < DU
IG	= 1, square crossection, = 0 circular crossection
EO	highest point on energy scale, usually source energy.

The SOURCE routine should generate all particles at one activation and place them on symbolic unit 10 and need not rewind the unit.

A number of simple source distributions are already built into the PROTOS 3 Monte Carlo program itself to provide for some frequently occurring, monoenergetic distributions of entry (narrow beam, centrally incident on plane surface at right angles with the surface, perpendicularly incident particles uniformly distributed over one plane exterior surface).

9. The PROTOS III program, written by C. Johansson, aided by E. K. Helwig, is a modified version of the original PROTOS program. Its theoretical description is given in Chapter 3. The main features of the PROTOS III program are that excitation, ionization, Coulomb scattering, range straggling and nuclear interactions are all included in the handling of proton transport. The neutron transport part is a straight-forward extension similar to the SUPER B program, 10. Data for nuclear interactions are obtained from tape 7. The results are compiled on a biography tape to be used for coupling the high-energy transport part of the code system into the low-energy part. A statistical analysis of the high-energy results may be performed separately, using the program PROUT 2, 11.

The computer program is written in FORTRAN IV language for the IBM 360/44 computer. The following information is given on input data preparation and on the interpretation of the output.

Composition of the Program (see flow charts in Figs. 4 and 5)

a. Main program

The main program is labelled PROTOS. Its purpose is to call the various subroutines.

b. Subroutines

PDATA. This subroutine reads the physical data, i.e. source energy (E_o), cut-off energy (E_n), atomic number of the slowing-down medium (Z) etc. The table of $(dE/\rho dx)_i$ is also read. A table of energy points between source and cut-off energies is prepared in one of three ways. For each energy step, four integrals are evaluated by Gaussian integration, giving values of $[s]_i$, $\chi^2_{c,i}$, $[\Delta s^2]$ and $\log [\chi^2_a]_i$ which are used to produce the four tables of $[s_i]$, $\chi_{c,i}$, $[\Delta s^2]$ and B_i. A table of the mean square polar deviation angle $\langle \omega^2 \rangle$ is the fifth table.

GDATA. This subroutine reads data specifying the geometry of the problem under consideration. The number of protons to be followed is also read here. No calculation is undertaken.

GEO. The source particles can be generated in two specified ways or by a customer supplied routine SOURCE. The source particles are all generated at the start and put on a disk tape. The particles can be protons and neutrons. The source tape is read and the particles are moved geometrically and in energy. If a nuclear interaction occurs the data at the instant before the collision is put on a file 1. When all source particles of one kind have been treated, a call is

made on the routine GENU. This routine generates secondary particles of both kinds and puts the neutrons on file 2. and protons on file 3. At the return from GENU to GEO the relevant one of the files 2 and 3 are rewound and used as source file. This can generate new tertiary particles and so on. One keeps treating particles of one kind as long as possible. This is in anticipating the time when there will be room in the core storage only for nuclear data for one kind of input particle.
The routine GEO also makes calls on STATI and OUT.

STATI is called after each geometrical move and tests if the particle has left the piece of matter. It also places data on the output binary tape. An entry OUT is the usual place to call when data is put on the output tape. See description of output tape.

RANDOM and RNORM give the random numbers.

GENU is the routine that generates the particles after nuclear interactions. Data before the collision are read from file 1 and secondary protons are put on file 3 and neutrons on file 2.

SOURCE is usually a dummy routine but the user can supply a routine that gives arbitrary source particles.

PUT is a blocking program.

IBAN is a block DATA routine.

c. Description of input data

Main program reads an indication I, format (I5)

I = 1 calls PDATA and returns to MAIN
I = 2 calls GDATA and returns to MAIN
I = 3 calls GEO and returns to MAIN
I = 6 reads 40 characters that are output when GEO begins and can be used as title.
I = 8, 9 or 10 must be used to stop the run so as to put an end mark on the binary output tape.

PDATA
The first card contains six data, format (2F5.0, 2I5, F5.0, I5, 28X, A4)
EO = Source energy in Mev
RO = Density in grams per cc
N = Number of arguments in the table of stopping power ($N \leq 200$)
M = Number of energy points in slowing down ($M \leq 100$)
ES = cut-off energy in Mev
KE = Indicator for kind of energy scale. KE = 1 gives M-1 logarithmic steps between EO and ES. KE = 2 gives M-1 linear steps and KE = 3 means that the

energy scale is supplied as data.
TEXT = Two characters identifying material.

The second card contains four data, format (2F5.0, 20X, 2I6)
Z: Atomic number of scattering atoms (or charge number of molecules).
CF: Constant parameter (fig. 6).
UNIF: Starting value for random uniform numbers.
RAN: Starting value for random normal numbers.

The third card contains one data, format (F10.0) the atomic (or molecular) weight.
The next cards contain a series of vectors, each vector beginning on a new card. The format is (7F10.0) throughout.
EN: N arguments (in Mev) for stopping power table ($EN_i < EN_{i+1}$).
DES: N values of the stopping power (in grams per cc) given at the arguments EN and in the same order as EN. If KE = 3 there follow cards for energy scale EK, M values and EK(I) > EK (I+1) and EO should be EK(1) and ES should be EK(M).

PDATA does not read any more data from the system input but does read nuclear data from a binary data tape. This binary tape will have been prepared before offline. The tape contains nuclear data for the specific composition that one wants to use. The first three values from the tape are z the nuclear charge, A the atomic weight, and the name of the composition. This is written on the system output as an indication of which tape the operator has put on.

GDATA reads just one card, format (2F10.0, 2I10).
DU = Total rod length in cm.
RU = Cylinder radius or half square side in cm.
IG = 0 cylindrical cross-section, = 1 square cross-section.
NT = Number of source particles.

GEO reads an indicator ISO, format (I5). If ISO = 4 GEO will call SOURCE to get source particles, ISO = 1 gives source particles incident at right angles to the input surface and along the axis. ISO = 2 gives input at right angles to the input face but randomly over the surface.
If ISO $\neq$ 4, GEO will read a card, format (7F10.0) for FAC which is the fraction of neutrons that is wanted in the source particles.

d. Description of Output

The output starts by reproducing the physical data. The succeeding columns, labelled EK, DS, and PRO contain
(1) the M energy values for the slowing down formalism (denoted E_i in chapter 3),

(2) M corresponding values of $[s_i]$ (see equation 3-13), and
(3) M values of $([\Delta s^2]_i)^{\frac{1}{2}}$ (see equation 3-14).

Then the remainder of the input data is reproduced.
GEO puts out what sort of source particles it works on: the started ones or secondary ones. One can also see the number of secondary particles that are generated from the nuclear interactions (calls PRIMS).

The program finishes by printing the number of low neutrons (<14.1Mev) that is on the biography tape. This will help in deciding if SUPER B should be used.

The last line of a successful run is THIS IS THE END.
No further information is put on the system output tape 6 but the histories are put on the binary output tape 4.

On tape 4 is put in binary X, Y, Z, ϕ, θ, E, IK and NSOU. When a new problem is started by calling GEO IK = 100 and when the run is ended IK = 10000. In all other records IK > 0 if the particle is a proton and IK < 0 for a neutron.

A new particle has |IK| = 4
A moved particle has |IK| = 1 if still inside.
A moved particle has |IK| = 2 if it just has passed boundary.
A particle before collision has |IK| = 3.
If a particle has passed the boundary |IK| = 2.
The values of X - - - E are the values the particle would have had if the material had extended all the way.
NSOU is the number of the ultimate ancestor of the particle, NSOU = 1, NT.

An example of a program that interpolates the values at the boundaries and gives the energy spectrum for penetrating particles and for the side leakage is given by PROUT.

Table 4-2
PROTOS III Output

```
TEXT ON DATA TAPE:  IDENT=E003, NAME=SI, DENSITY= 2.33
EO=185.0    RO=2.3280    NUMBER OF STEPS=100    Z=14.
CF= -5.20   E CUT OFF=2.0    AKK=1.100    AVD=0.49924E 23
INFORMATION FOR CALCULATIONS OF STOPPING POWER
I = 172.8    Z = 14.0000    A = 28.0860
LENGTH = 15.0, HALF SQUARE SIDE = 15.0, NT = 2000
185  MEV PROTONS ON SILICON

1663SECS FROM 491PRIMS                    139SECONDARY NEUTRONS
 977SECONDARY PROTONS                       9SECS FROM    7PRIMS
  55SECS FROM   19PRIMS                     7SECONDARY NEUTRONS
  33SECONDARY PROTONS                      74SECONDARY PROTONS
   2SECS FROM    1PRIMS                     3SECS FROM    1PRIMS
   2SECONDARY PROTONS                       2SECONDARY PROTONS
 708SECONDARY NEUTRONS                      1SECONDARY NEUTRONS
 211SECS FROM    7PRIMS                NUMBER OF LOW NEUTRONS IS 115
```

10. The SUPER B program, written by C. Johansson, is a modified version of the SUPER program described in reference 6.

The PROTOS III program is not useful at lower neutron energies where more detailed data is needed. If PROTOS III creates a neutron at a lower energy than 14 Mev it will not try to continue the slowing down process but will leave it on the biography tape. The SUPER B program reads and copies the biography tape and when it finds a neutron with energy below 14 Mev, it slows this neutron down past a preselected cut-off energy E_{th}, where a constant mean-free-path and absorption probability is used. The SUPER B program puts the biography of this on to the copy-tape so that the final result is an expanded biography tape in the PROTOS III format.

The slowing down of the neutron is done by the Standard Monte Carlo technique, i.e. Find the mean-free-path-length at this energy, select an actual pathlength from the exponential distribution, move the particle to the new point, check to see that it is still inside the body, find absorption probability, Russian roulette, find probabilities for different reactions with the different elements at this energy, select element and reaction, use the appropriate formula to get energy after reaction and scattering angle, transform to lab system, transform polar angle to direction cosines and you are ready for a new round trip by finding mean-free-pathlength and so on.. All the neutron data for the given compound is previously prepared on a data tape called 13 , Figures 2 and 3.

Neutron Data Tape: The "United Kingdom Neutron Data File (UKNDF)" is the source of this data. UKNDF is a library of evaluated neutron cross sections, initially compiled and evaluated at laboratories in many countries (England, France, Germany, Sweden etc.) and is the most up-to-date, complete, and readily available library of this nature. A general description of UKNDF is given in reference 5. Table 4-3 presents contents of the file.

A program INTE, written by A Henriksson, was used to pick out the appropriate elements from the UKNDF (or other similar) file, to interpolate in energy and to edit the data in a suitable form. The results are presently produced on punched cards in a format used as input for the R3B program 14 which prepared the data for arbitrary mixtures and compounds in a form suitable for Monte Carlo calculations. The R3B program was written by A. Henriksson. The final results of tabulated nuclear data for energies below 14 Mev, pertaining to the medium under consideration, were printed on magnetic tape 13. Data for the twelve elements and mixtures listed in Table 4-1 are given as part of the PROPER 3B code package already in the 11 format for direct use in conjunction with the Monte Carlo transport program. A large variety of possible materials are available for the low energy neutron transport calculation. If new materials or mixtures need to be added, contact M. Leimdorfer. It might be remarked at this point that a small

addition was made to the information coming from the UKNDF data file 16 by selecting parameters for evaporation model spectra in the continuum secondary energy part of inelastic neutron scattering and (n, 2n) reactions (6).

TABLE 4-3

Table of elements in the United Kingdom Neutron Data File, available as input to the R3-B program, producing neutron cross-sections in magnetic tape form for the SUPER B program.

Excerpt from Newsletter No. 5 (1967) of the Neutron Data Compilation Centre of the European Nuclear Energy Agency, Saclay, France.
Prepared by Lars Wallin

Report ref.	Element	Date	Author
AEEW M513	BE9	Mar 65	G. Doherty
AEEW R116	XE135	Jun 62	H.M. Sumner
AEEW R254	NA23	Apr 63	T.P. Moorhead
AEEW R351	H2O, D, D2O,HE4,PE BEO,B,B10,C,N,F,NA SI,CR,FE,NI,CD,XE135 PB,TH232,PU239, PU240	Jul 63	E.P. Barrington, A.L. Pope, J.S. Story
AEEW-M 414	U238	Dec 63	H.M. Sumner
AEEW-M 445	O,AL	Jul 64	D.C. King
AEEW-M 502	U235	May 65	R.G. Freemantle
AEEW-M 504	ZR	Sep 66	A.L. Pope
AEEW-M 714	PU241	Jan 67	G. Doherty
AWRE C-30/64	U236	Jul 64	K. Parker
AWRE C-37/64	U234	Jul 64	K. Parker
AWRE O-60/64	LI6	Jul 64	E.D. Pendlebury
AWRE O-61/64	LI7	Jul 64	E.D. Pendlebury
AWRE O-77/64	TI	Oct 64	S.M.Miller,K.Parker
AWRE O-78/64	HE3	Aug 64	P. Batchelor, K. Parker
AWRE O-79/64	PU239	Jan 65	A.C. Douglas, J.P. Barry
AWRE O-91/64	PU240	Jan 65	A.C. Douglas
AWRE O-100/64	U233	Jan 65	A.C. Douglas
AWRE O-101/64	PU241	Feb 65	A.C. Douglas
AWRE O-23/65	H	Jul 65	A. Horsley
Unpublished	AU		
"	CU		

AWRE C-55/65 GIVES CONTENTS OF UKAEA NUCLEAR DATA LIBRARY ASAT 15TH APRIL 1965 REVISED VERSION OF UKAEA NUCLEAR DATA LIBRARY RELEASED JANUARY 1967.

This description of the SUPER B routines refers to Figure 7.

MAIN. This reads the first record from the data tape and reads the description of the body, see below on data cards.

START. This routine reads the PROTOS biography tape until it finds a nuclear interaction for a neutron with energy below 14 Mev. When START does find a low energy neutron it runs down into the entry.

EXPEN which computes mean-free-path length, moves particles, absorption probability and does the Russian Roulette. If the neutron survives, the control goes to REAKT. If the particle is absorbed, control goes to START. EXPEN uses STATI and OUT to put information on the copied biography tape.

REAKT chooses reaction and element by calculating the corresponding probabilities. If the reaction is fission, the energy of the new particle and the lab scattering angle are computed in REAKT and control goes to REOR. If the reaction is not fission, control is given to the appropriate one of ELAST (elastic scattering), INELAST (inelastic scattering), NTVN (n, 2n).

ELAST starts by testing for isotropic scattering in the c.m. system. Otherwise it selects the angle from the distribution for the angle (at this energy and with this element). The c.m. angle is converted to the lab system and the resulting energy in the lab system is calculated. Control goes to REOR.

INELAST starts by testing the neutron energy to see if continuous or discrete energy loss is to be applied. If discrete, a level is chosen from the probabilities and the resulting lab energy is computed. The scattering is isotropic in the c.m. system. If the continuous part applies, the correct parameters for this element are chosen and an energy is drawn from the distribution, control goes to REOR.

NTVN gets its secondary energy with an even chance from one of two distributions of the same general form as in the continuous part of INELAST.

REOR Test if the new energy is below cut-off in which case control goes to START to search for a new particle. REOR also tests to see if a new record needs to be read from the data tape or if the new energy can be handled from the record already in core storage. REOR then calls CHANIL and when control returns to REOR it gives control to EXPEN.

CHANIL computes the new direction of travel (in x,y,z system) from the old direction and the scattering angle.

DATAIN finds the correct (in energy) record on the data tape when a change is needed.

STATI checks to see if the particle is still inside body or has left it. It also puts information for the new biography tape on the disk.

OUT is an entry to STATI when one just wants to put information for the biography tape on the disk.

When START reuses IK = 10000 on the biography tape, it backspaces one record and reads the SUPER B information from the disk onto the biography tape and puts a 10000 record at the end. The result is a new biography tape with the PROTOS 3 data undisturbed and with the old end marker replaced by SUPER B biography and a new end marker.

INPUT

Data card in the FORMAT (3F10.0, I10)

EMIN	cut-off energy
DU	Length of body
RU	Radius or half side of square
IG	= 1 square cross-section, = 0 circular

Data card in FORMAT (3F10.0)

ETH	"thermal" energy
PAAS	probability of absorption at ETH
ALTH	mean-free-path at ETH

Data tape with low energy neutron data on symbolic unit 13

PROTOS biography tape

Output

The input cards are reproduced and when the run has come to a correct stop FINISHED will be printed.

Enlarged biography tape is on PROTOS biography tape 12.

The biography tape, created by PROTOS 3 and SUPER B, contains the tape-recorded autobiography of the complete histories of the nucleons whose lives in the medium have been simulated by the Monte Carlo programs. The biography tape is analyzed statistically using a program PROUT 2 which calculates energy spectra of neutrons and protons that leak out through various surfaces of the absorber medium as well as energy distributions of energy absorbed ina given volume inside the absorber.

11. PROUT 2 was written by T. Tengstrand. PROUT 2 may use the biography tape any number of times for analysis of any quantity pertinent to the problem.

    PROUT 2 reads data from tape 12 in an internal code which contains coordinates, energies, kind of particles, information about the parent source particle and type of event (=KI, see page 18).

The program studies two bodies, each with six plane limiting surfaces; one outer surface, giving rise to statistics 1 (STAT 1) and one inner body, giving rise to statistics 2 (STAT 2).

Here we assume that the inner body is totally enclosed by the outer body.

When dealing with the outer body, routine STAT1 performs: Sorting of the particles with reference to 1) Kind of particle 2) Value of energy 3) Geometric point of escape.

When dealing with the inner body, routine STAT2 performs: Calculation of the energy loss for every original source particle. The energy losses are then sorted into energy intervals (EN(100), (SLASK(2000) with the number of entries = the number of original source particles, is used in the calculation.

PROUT 2 consists of one main program and 6 subroutines.

1. Main program PROUT 2
   This program administrates reading, writing, and calling of STAT 2.
2. Logical function TEST
   This program tests if the coordinates x, y, z (in the argument list) are within the body or not.
3. Subroutine FELUTS
   This program writes an error message giving an indication of the reason for the error.
4. Subroutine BAS
   This program places the different energies (called 'ESL' in the argument list) into different energy intervals (EN (i) - EN (i+1)) and counts the number of energies within every interval and places these numbers in the vector OUT.
5. Subroutine INSIDE
   This program calculates the intersection point(s) of the particle path with the surfaces of body. (The coordinates of the intersection point(s) are called AX(6), AY(6), AZ(6) in the argument list).
6. Subroutine STAT 1
7. Subroutine STAT 2

The value of the constant K 1

K 1 > 0	protons
K 1 < 0	neutrons
|K 1| = 1	the particle is inside the outer body
|K 1| = 2	outside the outer body
|K 1| = 3	nuclear reaction
|K 1| = 4	start of a new particle
|K 1| = 100	new data set
|K 1| = 10000	the end of the run

Data Cards

A. NTLPA, IOUTPT, N, IUTSKR, (EN(i), i = 1, N)
FORMAT (4I5, /(8F10.0))
B. A1, B1, C1, D1,A2, B2, C2, D2, (Dimension A1(6), B1(6), B1(6),...)
FORMAT (6F10.0)

Meaning of variables

A. NTLPA = the number of source particles (limit $\leq$ 2000)
IOUTPT = 1 causes printing of the biography tape.
N = the number of energy points (the number of energy intervals 'N1O' = N-1)
IUTSKR = constant
IUTSKR 0 'STAT 1' is performed (outer body only)
IUTSKR = 0 'STAT 1' and 'STAT 2' are performed (both bodies)
IUTSKR 0 'STAT 2' is performed (inner body only)
EN = the energy scale E(I) E(I+i)
B. Here the coefficients of the equation of the plane are read ($\underline{A}X + \underline{B}Y + \underline{C}Z + \underline{D} = 0$)

For the outer body A1, B1, C1, D1 and (must be the same as PROTOS III outer body)
For the inner body A2, B2, C2, D2, the reading is done according to the following:
All six A1-coefficients on the first card
All six B1-coefficients on the second card etc.

One point $P_o(x_o, y_o, z_o)$ and two vectors, not parallel, and $v_2 = (\alpha_2, \beta_2, \gamma_2)$ gives the coefficients A, B, C, and D in the equation

If you know three different points in the plane $P_o(x_o, y_o, z_o)$, $P_1(x_1, y_1, z_1)$ and $P_2(x_2, y_2, z_2)$, you can get the vectors from

$$\underline{v}_1: \quad (x_1 - x_o, y_1 - y_o, z_1 - z_o), \quad \underline{v}_2: \quad (x_2 - x_o, y_2 - y_o, z_2 - z_o)$$

$$A = \begin{vmatrix} \beta_1 & \beta_2 \\ \gamma_1 & \gamma_2 \end{vmatrix}, \quad B = \begin{vmatrix} \gamma_1 & \gamma_2 \\ \alpha_1 & \alpha_2 \end{vmatrix}, \quad C = \begin{vmatrix} \alpha_1 & \alpha_2 \\ \beta_1 & \beta_2 \end{vmatrix}, \quad D = - \begin{vmatrix} x_o & \alpha_1 & \alpha_2 \\ y_o & \beta_1 & \beta_2 \\ z_o & \gamma_1 & \gamma_2 \end{vmatrix}$$

When numbering the planes, refer to Figures 4-8 and 4-9.

SAMPLE PROBLEM

A block of silicon, 30X30X15 cm in size, is bombarded by a beam of monoenergetic protons. The beam has a crossection of one square mm and entered the silicon at the center of the 30X30 face of the block traveling parallel to the Z-axis (see Figure 4-9). The history of 2000 monoenergetic (E_o = 185 MeV) were studied.

Table 4-2, page 4-13, contains a listing of the nuclear reaction data pertinent to the entire block of silicon. Of the 2000 primary protons, 491 had nuclear reactions, creating a total of 1663 secondary particles (977 protons - 686 neutrons). The history of the 977 secondary protons revealed that 19 reacted to produce 55 tertiaries (33 protons - 22 neutrons), and in turn, one tertiary proton reacted and produced 2 fourth generation protons.

Counting all generations of proton - silicon reactions, a total of 708 neutrons had been created thus far in the study. Of these, 93 reacted with silicon nuclei to produce another 211 secondary particles (139 neutrons - 72 protons). Continuing the chain of reactions, 7 of the 139 neutrons reacted to produce 7 neutrons and 2 protons.

An additional 74 protons were created in the neutron-silicon reactions. These produced 2 more protons and one more neutron, ending the chain. The entire history of each primary proton includes the history of all secondaries created after its initial nuclear reaction, and all of this information is stored on Biography Tape 12.

The initial printout of the PROTOS 3 generated data also gives the number of neutrons which have either been created with or slowed to an energy of less than 14 Mev. In the sample problem, the number of such neutrons was 115. The investigator now may use SUPER B to take these neutrons and carry them down to either thermal energy or to exit from the medium. When the neutrons are slowed down past a preselected cut-off energy E_{th}, 0.025 eV $< E_{th} <$ 14 Mev, they are treated as a one-velocity thermal group with a fixed mean-free-path and absorption probability with isotropic collisions in the laboratory system. When a thermal neutron flux is desired, E_{th} should be set near about 0.1 eV and appropriate numbers for the mean-free-path and thermal absorption probability should be entered into the SUPER B input. By setting the absorption probability equal to 1, termination may be achieved at any value of E_{th}, chosen inside the above interval. The SUPER B program adds information on the low energy parts of neutron histories to the biography tape.

PROUT 2 is used to read the data required to analyze a problem. The investigator selects the range of energy and the energy intervals (not to exceed 100) of interest. The energy range from 0 to 185 Mev was divided as follows: 0 to 16 Mev in steps of 1 Mev; 16 to 58 Mev in steps of 2 Mev; 58 to 70 in steps of 4 Mev; and 70 to 185 in steps of 5 Mev, in the example given in Table 4-4. The first column of Table 4-4 gives the energy interval.

The next six columns give data concerning the particles which have escaped from the outer body and the energy interval indicates the energy of the escaping particle. Thus one neutron excaped through the end of the silicon block and it had an energy between 165 - 170 Mev. The tape carries the exact energy, location and angle of escape. A total of 395 neutrons and only 2 secondary protons escaped.

NOTE: In multislab calculations, the outer body can be a slab and the biography tape can become the new SOURCE data tape to permit change of medium yet continue the history of a given original spectrum of particles.

Data related to the inner body is obtained using PROUT 2. The investigator selects the size, shape and position of the inner body with the restriction that it must be totally inside the outer body.

The column headed NR ABS lists the number of primary protons which deposited energy within each energy interval. The energy absorbed in the inner body from a single primary proton is the differences between the sum of the energies of all the protons and neutrons (having the same parent primary proton) entering the body and the sum of the energies of all those which have left it, minus the energy equivalent of any increase in rest mass that took place in nuclear reactions within the volume.

The column headed E ABS gives the energy absorbed as defined above. In the sample problem, 65 primary protons had nuclear reactions which produced energy absorbed in the chosen inner body (either from the primary or the combination of primary and secondaries or from the secondaries) and the distribution of this energy is given in Table 4-4. Another 173 primary particles either made no contribution toward the energy absorbed or had more energy leaving the volume than entered, indicating a deficit of 461.4 Mev for the 173 primaries after nuclear reactions.

The remainder, 1761 primary protons, did not have nuclear reactions but deposited energy by ionization and excitation. The energy spectrum of this group may be obtained by dividing the energy range from 9.5 to 13.0 Mev into 35 intervals and then analyzing the resulting peak.

The total energy absorded in the cubic centimeter of silicon was calculated to be 23,426.1 Mev. Of this, 19,863.9 Mev was absorbed from 1761 protons that had not undergone a nuclear reaction. The remainder, 3,562.2 Mev was absorbed from protons or neutrons which had had a reaction.

References:

1. H. W. Bertini, Phys. Rev. Vol. 131, No. 4 (1963) 1801, with erratum Phys. Rev. Vol. 138, No. AB2 (1965)

2. M. Leimdorfer et al; ORNL-4002 (1967)

3. A. Henriksson et al: "The CASEVA Program", FOA Report (to be issued)

4. H. W. Bertini, ORNL-3383 (1963) Chapter III.I

5. J. S. Story et al, Proc. of the Third International Conference on the Peaceful Uses of Atomic Energy, Vol. 2 (1965) 168

6. M. Leimdorfer, FOA Report FOA 4 A 4366-411 (1964)

7. W. Guber et al, Trans. Am. Nucl. Soc. 9, No. 2 (1966) 358

Table 4-4

SAMPLE PROUT OUTPUT

PROUT2 VERSION 1.00 SUBPROGRAM TO PROTOS

NTPLA 2000IOUTPT 0 IUTSKR 0
2 Bodies, Each with 6 Plane Sidesurfaces
(The equation used for the planes is A*X+B*Y+C*Z+D=0)

The Coefficients to the Equations
The Outer Body

Plane No.	A	B	C	D
1	0.0	0.0	1.0000	0.0
2	0.0	0.0	1.0000	-15.0000
3	1.0000	0.0	0.0	15.0000
4	1.0000	0.0	0.0	-15.0000
5	0.0	1.0000	0.0	15.0000
6	0.0	1.0000	0.0	-15.0000

The Inner Body

Plane No.	A	B	C	D
1	0.0	0.0	1.0000	-5.0000
2	0.0	0.0	1.0000	-6.0000
3	1.0000	0.0	0.0	0.5000
4	1.0000	0.0	0.0	-0.5000
5	0.0	1.0000	0.0	0.5000
6	0.0	1.0000	0.0	-0.5000

	Outer Body						Inner Body	
EN	Neutr. Side	Prot. Side	Neutr. End	Prot. End	Neutr. Refl.	Prot. Refl.	NR ABS	E ABS
170-165			1.					
155-150			1.					
150-145			2.					
145-140			3.					
140-135			2.				6.	820.9
135-130			3.				5.	667.1
130-125	1		3.				1.	127.0
125-120			2.					
120-115			3.				1.	119.5
115-110			4.				1.	112.9
110-105			3.				2.	211.9
105-100	2		2.				1.	102.8
100- 95	1		2.				1.	99.9
95- 90			6.				1.	93.1
90- 85	1		4.				3.	262.9
85- 80	1		8.					

EN	Outer Body						Inner Body	
	Neutr. Side	Prot. Side	Neutr. End	Prot. End	Neutr. Refl.	Prot. Refl.	NR ABS	E ABS
80 - 75			7.					
70 - 66	2		5				1	67.2
66 - 62	1		12					
62 - 58	2		12	1			1	58.2
58 - 56			3	1				
56 - 54	1		4				1	54.3
54 - 52	3		2					
52 - 50			1					
50 - 48	2		6					
48 -			1					
46 - 44			3					
44 - 42	2		1					
42 - 40			3					
40 - 38	1		5					
38 - 36	3		3				1	36.8
36 - 34	1		5					
34 - 32			4				1	32.2
32 - 30	1		4				1	30.2
30 - 28	1		5				2	58.0
28 - 26	1		8		1			
26 - 24	1		5		1		3	75.7
24 - 22	4		3		1		1	23.8
22 - 20	2		11		1			
20 - 18	3		11		1		2	36.1
18 - 16	4		5				2	34.3
16 - 15	2		5		1		2	31.2
15 - 14	1		6				4	58.4
14 - 13	4		5		1		1	13.3
13 - 12	1		1		1		124	1521.5
12 - 11	1		2		2		1127	12871.6
11 - 10	2		3		2		510	5470.8
10 - 9.0	5		4		5		4	39.5
9.0- 8.0	4		2		5		2	16.9
8.0- 7.0	7		7		2		3	22.8
7.0- 6.0	6		6		4		2	13.8
6.0- 5.0	9		5		7		2	11.5
5.0- 4.0	17		10		10		1	4.8
4.0- 3.0	15		15		9		1	3.6
3.0- 2.0	13		18		14		1	2.1
2.0- 1.0							2	2.9
1.0- 0							173	-461.4

Total absorbed energy is 23426.1

Table 4-4 continued

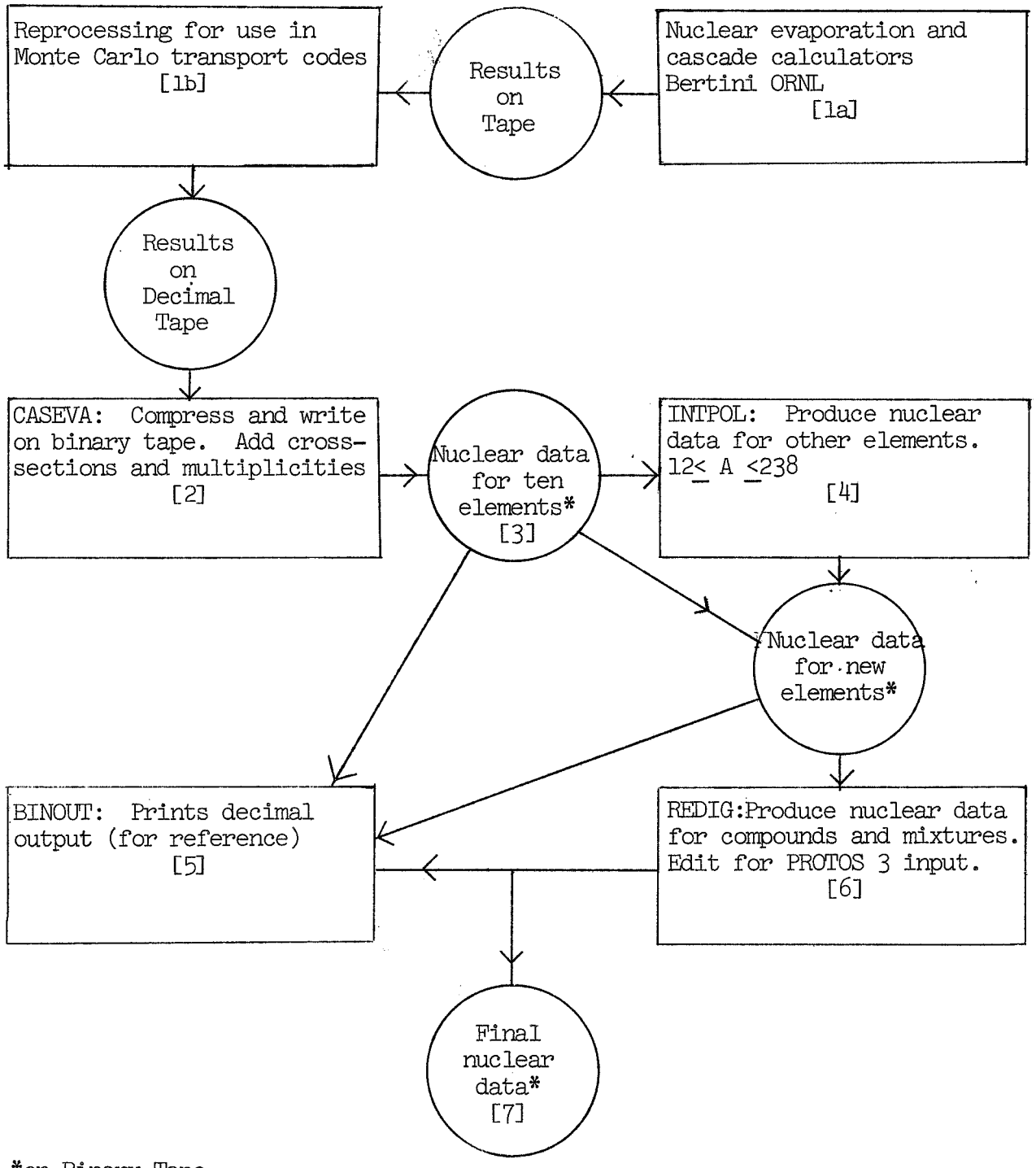

*on Binary Tape

Figure 4-1

Proper 3B System: Nuclear Data Preparation

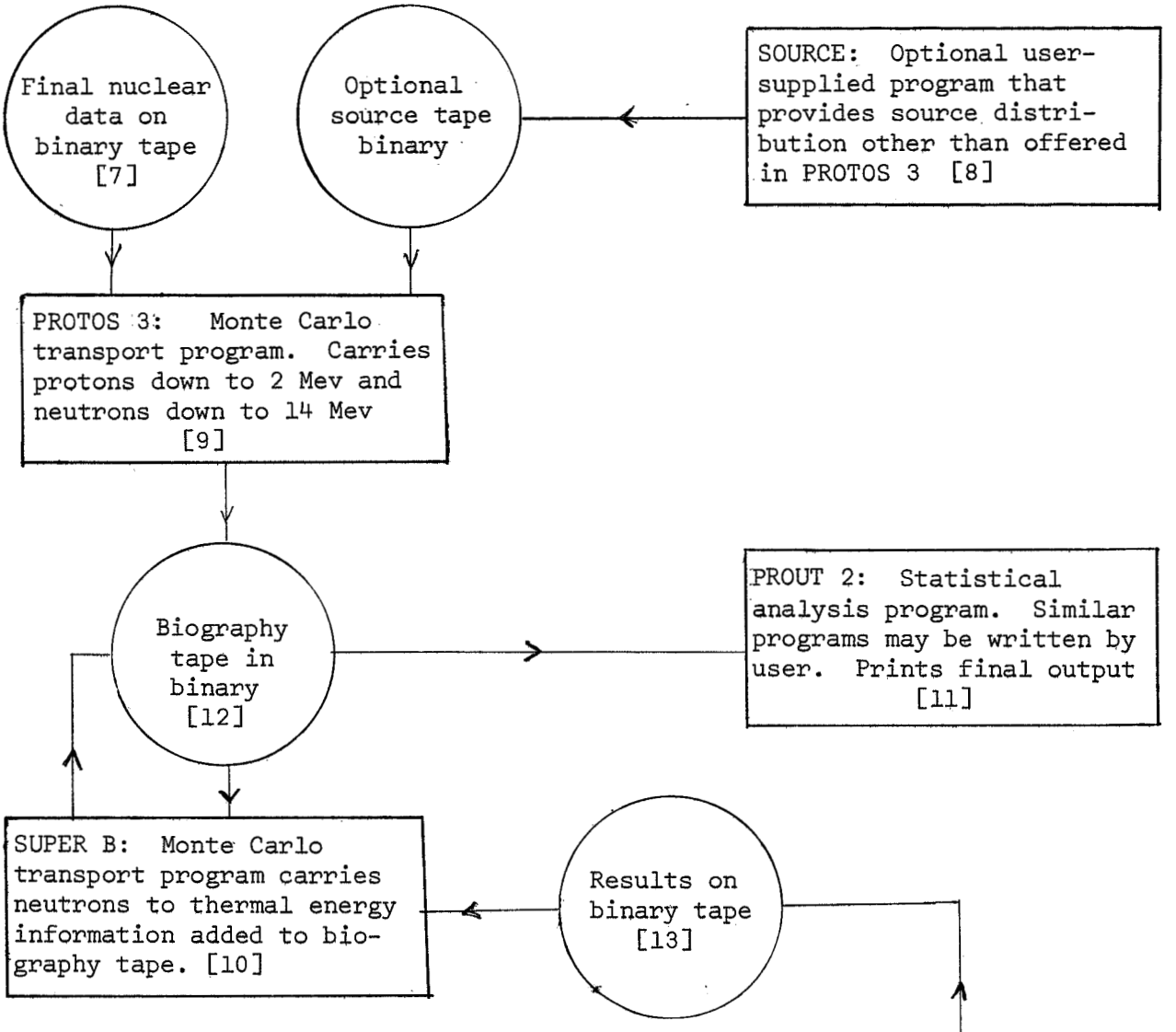

Figure 4-2: Main Program Flow Chart

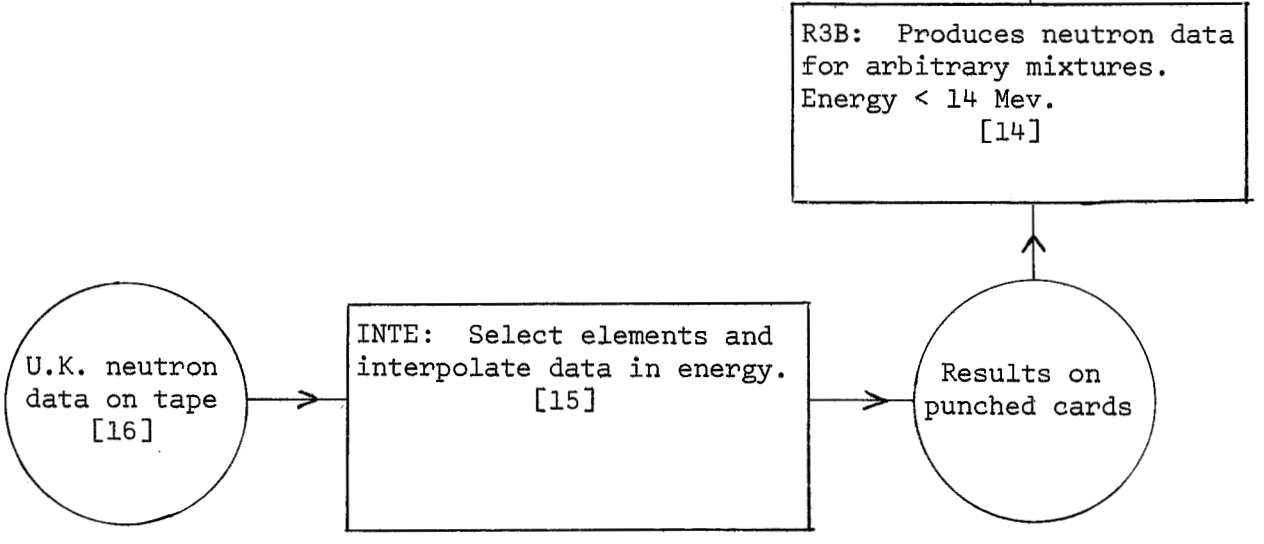

Figure 4-3: Preparation for Data Input to Super B ([14], [15], and [16] not part of Proper 3B).

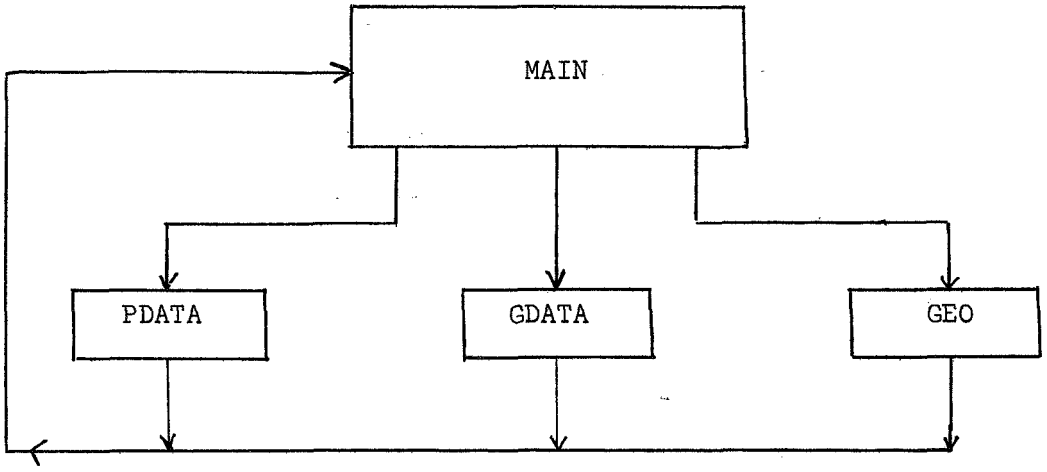

Figure 4-4

PROTOS III Main Programs and Subroutines Flow Chart

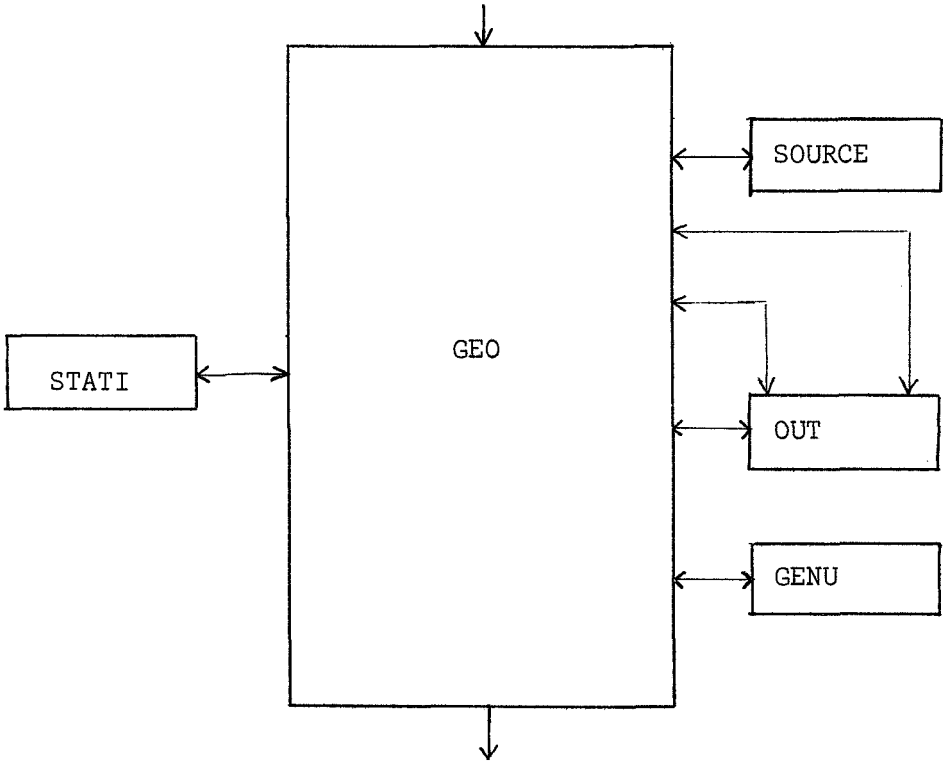

Figure 4-5

GEO Subroutines Flow Chart

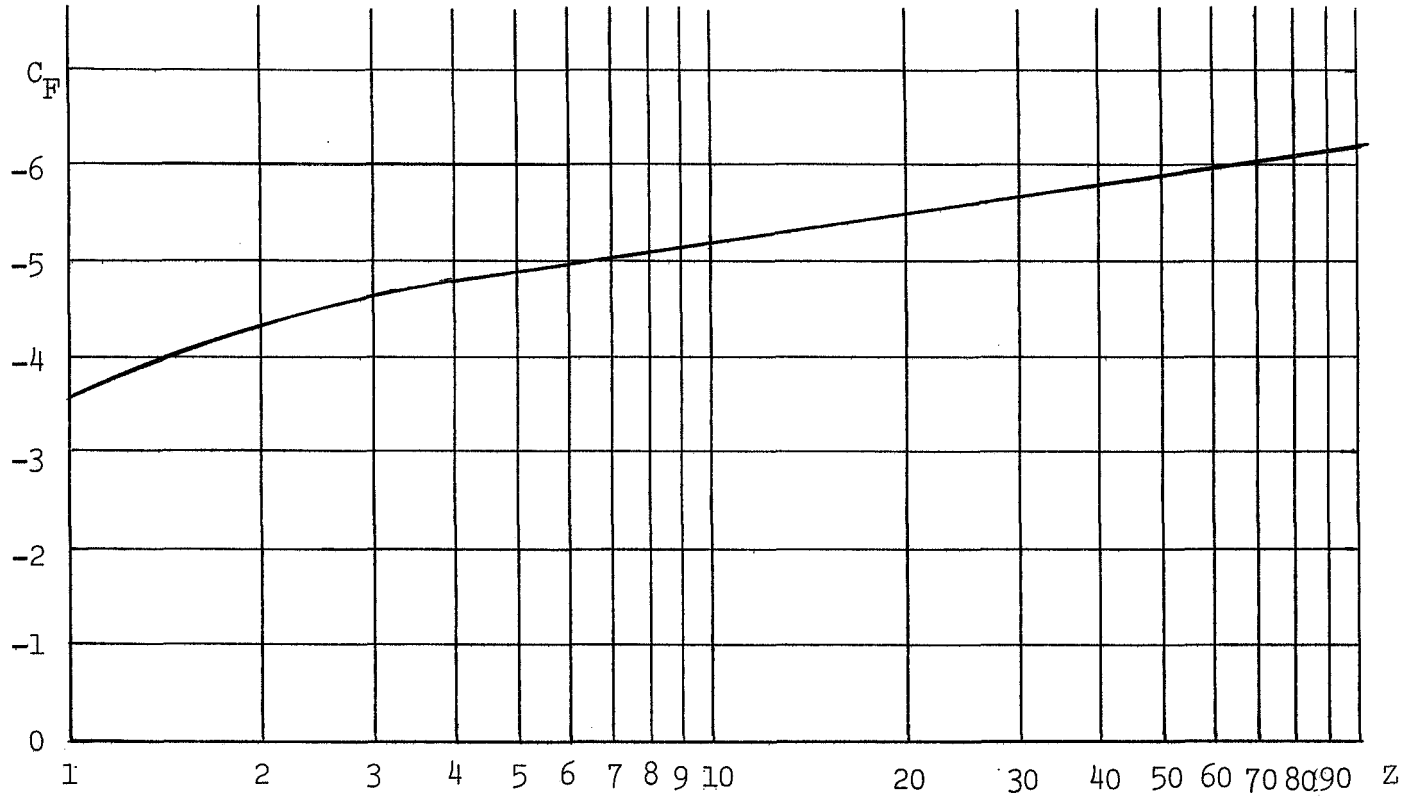

Figure 4-6

Variation of Parameter C_F with Atomic Number Z

The following values for C_F were used in this report.

Atomic Number	C_F
4	-4.80
6	-4.94
13	-5.20
14	-5.25
26	-5.57
29	-5.61
82	-6.07

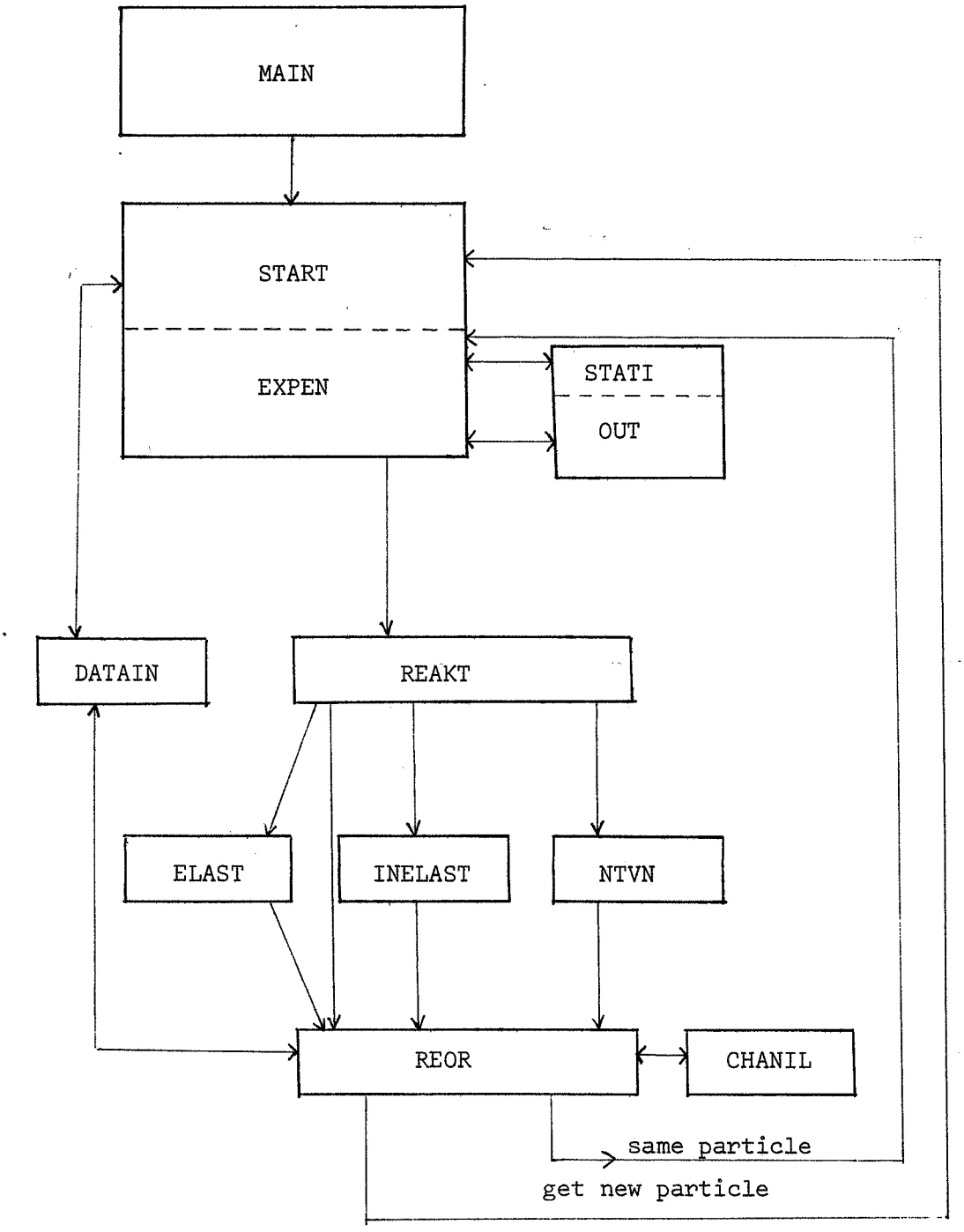

Figure 4-7

Super B Subroutine Flow Chart

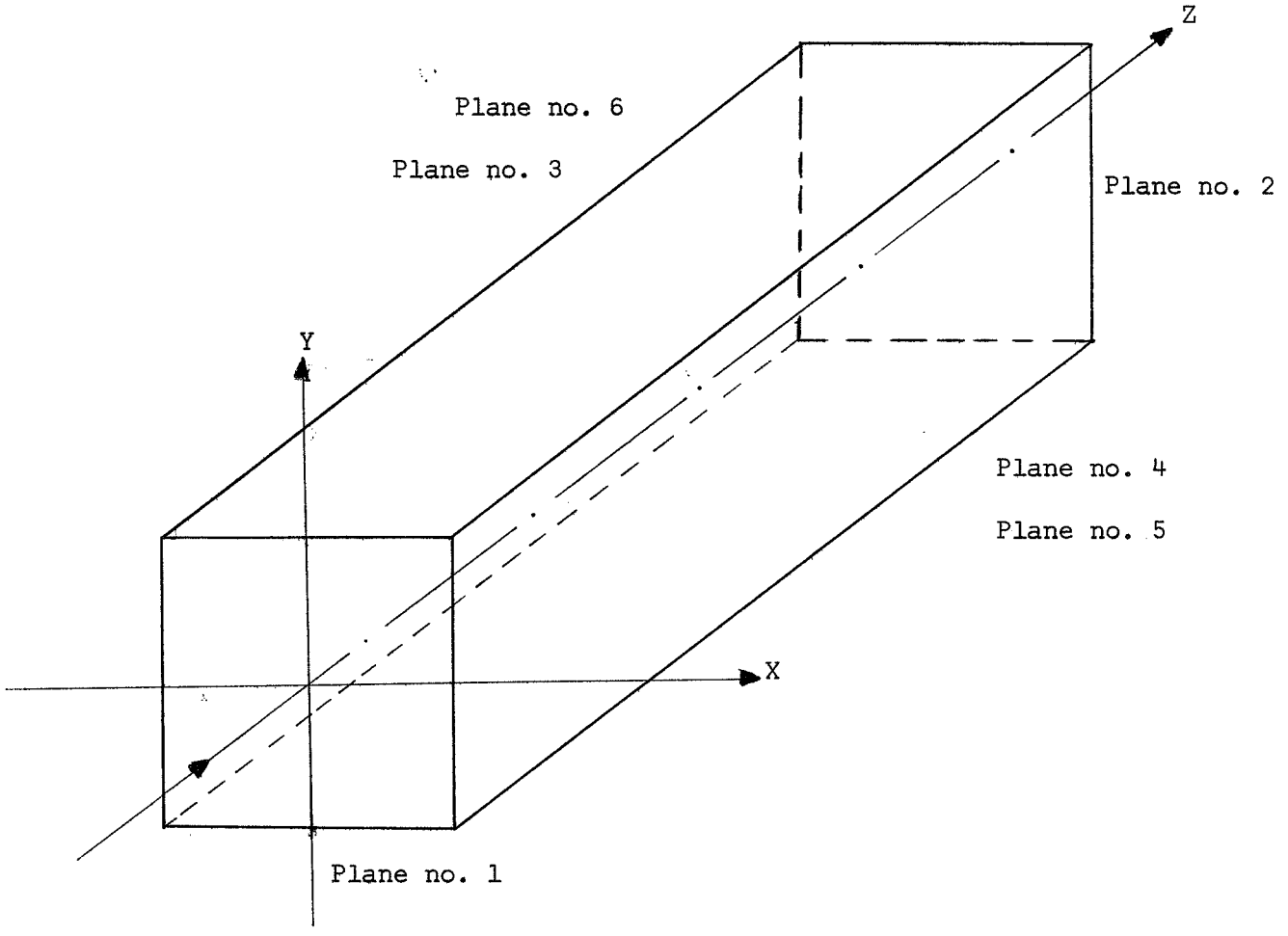

In the output listing

Plane no. 1 (front) is named 'REFL'. (means reflected)
Plane no. 2 (back) is named 'END'
Plane no. 3
Plane no. 4 named 'SIDE'
Plane no. 5
Plane no. 6

Figure 4-8

Numbering of the Planes

The Outer Body

Figure 4-9

Coordinate System: The Inner and Outer Bodies

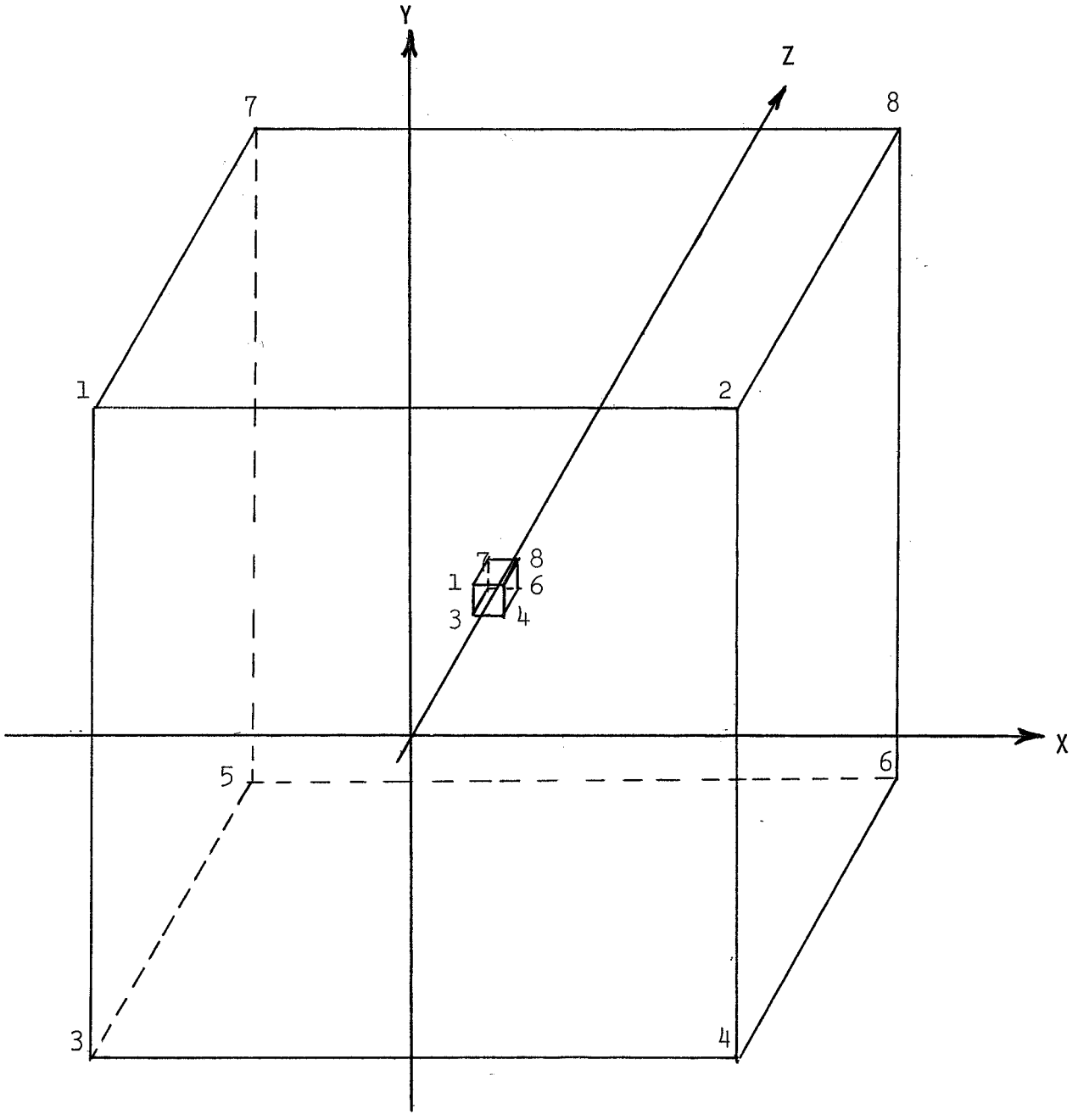

Coordinates

Location	Outer Body	Inner Body
1	(-15, 15, 0)	(-.5, .5, 5)
2	(15, 15, 0)	(.5, .5, 5)
3	(-15, -15, 0)	(-.5, -.5, 5)
4	(15, -15, 0)	(.5, -.5, 5)
5	(-15, -15, 15)	(-.5, -.5, 6)
6	(15, -15, 15)	(.5, -.5, 6)
7	(-15, 15, 15)	(-.5, .5, 6)
8	(15, 15, 15)	(.5, .5, 6)

CHAPTER 5

DEPTH DOSE DISTRIBUTION PRODUCED BY TRANSPORT OF 185 MEV PROTONS THROUGH SILICON

by George W. Crawford

Assume monoenergetic protons (E_o=185.0 MeV) concentrated in a beam having a cross section of one square millimeter, traveling in the positive Z direction parallel to the Z-axis. The protons enter a block of pure silicon at a spot centered on the face of the silicon, defined to be the origin of an X, Y, Z coordinate system. The block is oriented so that the front surface of the block is the X-Y plane at Z=0. For two of the three runs reported here, the block has an X-Y crosssection of 30X30 square centimeters. For the third run, the crosssection is reduced to 1X1 square centimeters.

Due to the limited storage capacity of the IBM 360-44 computer, the number of protons which can be programmed is limited. This limitation is overcome by changing the starting random numbers. If the starting numbers are the same, the program will duplicate a previous set of data. If they are different, the result is as a continuation of the earlier run and the results can be added for better statistics. In Table 5-1, the initial results of three runs are given. Runs 1 and 2 differ only by the random number used as the starting random number. Runs 2 and 3 differ only by the size of the X-Y cross section.

	Run No. 1	Run No. 2	Run No. 3
Length of silicon block (cm)	15	15	15
X-Y cross section of block (cm^2)	30X30	30X30	$\frac{1}{2}$X$\frac{1}{2}$
No. of starting protons	2000	2000	2000
Starting Random Numbers			
Gaussian	1198898385	409301248	409301248
Uniform	123456789	161738534 4	161738534 4
No. of starting protons having nuclear interactions	498	500	488
These produced: neutrons	701	705	729
protons	1013	1021	1013
No. secondary protons having nuclear interactions	19	12	11
These produced: neutrons	20	13	11
protons	33	19	19
No. of tertiary protons having nuclear interactions	0	1	0
These produced: neutrons		1	
protons		2	
No. of neutron created so far	721	719	740
having nuclear interactions	107	104	11
These produced: neutrons	170	151	21
protons	91	107	7
No. of these neutrons having nuclear interactions	8	9	0
These produced: neutrons	10	12	
protons	4	3	
No. of neutron produced protons	95	110	7
having nuclear interactions	0	2	0
These produced: neutrons		2	
protons		3	
No. of neutrons (E <14 MeV) in block	133	115	5

TABLE 5-1: Tabulation of Nuclear Interactions Occurring Within Silicon Block

The number of primary protons interacting in runs 1 and 2 was almost the same, 498 (1) as compared to 500 (2). The total number of secondary protons created was nearly the same, 1141 (1) and 1155 (2). Each had nearly the same number of neutrons created, 901 (1) and 883 (2). Using PROUT to determine the number of protons escaping from the large block, the count was 1 with 36 - 38 MeV energy for run 1 and 2 with 56 - 58 MeV energy for run 2. Other variations are revealed by comparing the distribution of energies of the neutrons which escaped from each block.

Energy Band (MeV)	Run Number 1			Run Number 2		
	Side	End	Front	Side	End	Front
170 - 160		1			1	
160 - 150		7			1	
150 - 140		2			5	
140 - 130		3			5	
130 - 120		5			5	
120 - 110	2	7			7	
110 - 100		7		2	5	
100 - 90	1	9		1	8	
90 - 80	1	6	1	2	12	
80 - 75		5			7	
75 - 70		11			8	
70 - 66	4	7		2	5	
66 - 62		4		1	12	
62 - 58		5	1	2	12	
58 - 54	3	3		1	7	
54 - 50		9			3	
50 - 46	1	5		2	7	
46 - 42	6	12		2	4	
42 - 38	1	8	1	1	8	
38 - 34	1	7	2	4	8	
34 - 30	1	9	2	1	8	
30 - 26	5	10		2	13	1
26 - 24	3	6		1	5	1
24 - 22	3	8	1	4	3	1
22 - 20	4	6	1	2	11	1
20 - 18	4	3	1	3	11	1
18 - 16	4	4	2	4	5	
16 - 15	2	2	2	2	5	1
15 - 14	8	7	3	1	6	
14 - 13	4	5	1	4	5	1
13 - 12	1	5	1	1	1	1
12 - 11	2	1	2	1	2	2
11 - 10	7	10	1	2	3	2
10 - 9	3	6	5	5	4	5
9 - 8	1	9	5	4	2	5
8 - 7	11	6	5	7	7	2
7 - 6	10	9	7	6	6	4
6 - 5	3	5	6	9	5	7
5 - 4	9	12	9	17	10	10
4 - 3	16	12	14	15	15	9
3 - 2	25	23	25	13	18	14
2 - 0	0	0	0	0	0	0
Total	146	281	98	124	275	68

Table 5-2: Energy Spectrum of Neutrons Escaping From Silicon

In comparing the energy spectrum of histories in the first centimeter of the block, other differences appear. The inner volume was selected to be that cubic centimeter located at a depth of 0.001 cm from the front and centered on the Z-axis. In runs 1 and 2, the same number of protons, 43, had nuclear interactions. The energy lost by ionization and excitation was the same, i.e., 1957 of the 2000 protons deposited 17,705 MeV of energy. But the nuclear reactions deposited different total energies; 31 reactions left 2,277.2 MeV energy and 12 reactions removed 799 MeV more than they deposited in run 1. In run 2, 33 of the reactions deposited 2,640.1 MeV and 10 removed 871.5 MeV more energy than they imparted. The spectrums are compared in Table 5-3.

Nuclear Interactions				Ionization and Excitation			
Run Number 1		Run Number 2		Run Number 1		Run Number 2	
Number of Protons	Energy Absorbed	Number of Protons	Energy Absorbed	Number of Protons	Energy Absorbed	Number of Protons	Energy Absorbed
1	182.4	2	365.9	1	10.7	Steps of 1.0 MeV	
		1	171.8	7	73.2		
3	491.5	1	167.1	17	174.7	56	569.4
3	458.8			37	373.4		
		1	147.1	273	2650.2		
		2	274.3	Energy Steps of 0.1 MeV			
1	129.0			97	916.4		
		1	120.2	129	1205.4		
2	232.3	1	118.0	134	1239.7		
		3	309.5	161	1472.9	982	9192.5
		1	93.5	145	1313.0		
1	86.9	2	172.1	179	1602.3		
1	76.4	1	78.1	150	1327.0		
		1	69.2	158	1382.8	893	7734.8
		1	66.4	123	1064.0		
1	65.1			121	1035.0		
1	59.9	1	59.4	Energy Steps of 0.5 MeV			
1	56.7	2	110.4	207	1723.2		
		1	53.0	18	141.1	26	204.2
		1	50.1	1957	17705	1957	17700.9
1	47.2	1	48.9				
2	87.2	1	45.3				
1	39.3	1	35.2				
1	32.8						
1	30.5						
3	87.6	1	28.3	Total Energy Absorbed in cm^3 of silicon			
1	22.5						
1	21.1	1	20.3	Run 1: 19,982.5 MeV			
1	18.5			Run 2: 20,349.9 MeV			
1	16.1						
1	13.1	1	13.2				
		1	12.3				
2	22.3	1	11.0				
		1	5.3				
		1	3.8				
10	-799.0	10	-871.5				
41	2277.2	43	2640.1				

Table 5-3: Energy Spectrum of Energy Absorbed in Cubic Centimeter of Silicon Located at Front of Block with Beam Centered..

Other differences appear between the two histories in the final centimeter of the path of the proton beam. The inner volume was selected to be that cubic centimeter centered on the Z-axis and located at a depth of 11.30 to 12.30 centimeters from the face of the silicon block. In run 1, a total of 838 of the original 2000 protons were missing from the beam in the final centimeter of path. In run 2, 820 protons were missing. That is, about 58% of the protons on the original beam were still in the spread beam at the end of the penetration. The large volume is used for this example as only about 7% of the original protons remained in an inner volume having the crosssection of the original beam. Nuclear interactions account for approximately 58% of the protons lost, large and multiple small angle scattering account for the remaining 42% of the 838 protons missing from the large volume. Statistical variations between two different runs of 2000 each are rarely greater than 2% and are usually less.

	Run 1		Run 2	
	Number of Protons	Energy Absorbed	Number of Protons	Energy Absorbed
48-46	1	47.4	1	46.3
46-44	59	2,624.6	58	2,584.2
44-42	178	7,635.6	179	7,699.7
42-40	235	9,657.5	212	8,688.1
40-38	215	8,378.1	246	9,614.5
38-36	138	5,110.0	152	5,616.1
36-34	91	3,195.1	102	3,580.6
34-32	53	1,759.9	57	1,881.5
32-30	36	1,115.8	30	930.9
30-28	10	289.9	15	935.6
28-26	6	163.2	9	241.8
26-24	10	250.7	9	227.0
24-22	7	159.5	3	69.9
22-20	12	250.9	10	213.9
20-18	10	188.8	9	173.5
18-16	9	151.3	6	101.1
16-14	8	120.6	9	136.1
14-12	13	169.6	6	78.0
12-10	12	128.6	13	142.5
10-8	7	63.6	17	151.0
8-6	7	51.7	12	83.7
6-4	18	88.9	10	50.4
4-2	13	40.3	8	22.5
2-.5	11	16.0	6	7.5
Escape	2	-25.7	1	-39.5
Sum	1162	41,725.8	1180	42,776.2
Missing	838		820	
Total	2000		2000	

Table 5-4: Spectrum of Energy Absorbed in Cubic Centimeter of Silicon Located at a depth of 11.30 to 12.30 centimeters and centered on the Z-axis

Depth in Silicon Rod	0-1 cm		1-2 cm		2-3 cm		5-6 cm		10-11 cm		11.3 - 12.3 cm	
Energy Band (MeV)	Number	Energy (MeV)	Number	Energy (MeV)	Number	Energy (MeV)	Number	Energy (MeV)	Number	Energy (MeV)	Number	Energy (MeV)
NUCLEAR INTERACTIONS												
185-160	4	673.9	4	724.6	8	1,359.3						
160-140	3	458.8	2	288.8	7	1,085.0						
140-120	1	129.0	3	410.7	7	902.6	12	1,614.0				
120-100	2	232.3	6	636.7	7	789.0	5	547.1				
100-80	1	86.9	9	811.8	3	263.1	5	455.9				
80-60	2	141.5	3	198.2	5	371.4	4	384.1	23	1,559.7	1	68.4
60-40	5	251.0	3	156.3	3	120.3	2	112.5	8	365.1	1	47.4
40-	13	303.8	7	204.6	5	185.4	20	430.0	14	437.3		
Sum	31	2,277.2	37	3,421.7	45	5,076.1	48	3,443.6	45	2,362.1	2	115.8
IONIZATION INTERACTIONS												
46-42											237	10,260.2
42-38											450	18,035.5
38-34											129	8.305.1
34-30											89	2,875.7
30-26											16	452.1
26-22									71	1,601.0	17	410.2
22-21									271	5,800.7	4	85.1
21-20									480	9,822.7	12	250.9
20-19									346	6,768.5	4	77.7
19-18									72	1,344.2	6	111.1
18-14									36	575.3	17	271.9
14-12					37	443.7	125	1,534.8	7	88.7	13	169.6
12-11	2	22.3	18	201.3	376	4,211.2	1127	12,871.6	7	81.2	4	45.2
11-10	62	632.0	349	3,584.2	631	6.443.5	510	5.470.8	4	41.0	8	83.4
10-9	939	8,797.6	994	9,368.6	524	4,883.3	4	39.5	12	114.2	3	28.7
9-8	938	8,134.3	515	4,420.5	295	2,426.0	2	16.9	8	67.2	4	34.9
8-6	18	141.1	46	357.7	16	116.1	5	36.6	13	88.5	9	51.7
6-4							3	16.3	8	38.8	10	88.9
4-0					3	8.2	4	8.6	23	54.6	28	56.3
Sum	1956	17,727.3	1922	17,929.3	1882	18,532.0	1780	19,995.1	1358	26,486.6	1178	41,861.0
Leakage	10	-799.0	41	-1,249.6	63	-1,171.6	172	-461.4	597	-64.4	820	-30.5
Total	2000	19,205.5	2000	20,101.4	2000	22,436.5	2000	22,977.3	2000	28,784.3	2000	41,946.3

Table 5-5: Energy absorbed per cubic centimeter from protons (E_o = 185 MeV) at various depths inside silicon block, absorbing volumes centered along the Z-axis (straight-ahead penetration path).

The proper 3B system permits detailed study of the energy exchange between the incident protons and the target material. Table 5-1 contains the results of three studies in which a beam of 2000 protons, each having an incident energy of 185 MeV, penetrated a block of silicon. Selecting run number 1 as a representative, the spectrum energy absorbed in each of the six different inner volumes are presented in Table 5-5. Each inner volume is 1 x 1 x 1 cm^3 oriented so that the volume is centered in the Z-axis and the "straight-ahead" penetration path enters the center of a 1 x 1 cm^2 face. The location of the cubic centimeter volume is given by the Z-coordinates of its face and rear. For example, the 0-1 cube has its face x-y plane centered in the beam at z=0 (front surface of the block) and its rear x-y plane one centimeter deep in the block. The one source millimeter beam was assumed to enter the block with all protons traveling parallel to the z-axis

In this first inner volume, 31 protons had nuclear reactions depositing 2,277.2 MeV of energy. Some 1956 protons underwent multiple ionization and exictation collisions, 18 depositing less than 8 MeV and 64 more than 10 with a 9.06 MeV most probable value for the energy absorbed. The distribution between energy absorbed from nuclear interactions, multiple ionization collisions, and that lost by leakage is shown in Table 5-6.

Depth in Block (cm)	Energy Nuclear Interactions (Percent)	Absorbed Ionization Collisions (Percent)	Energy Removed Leakage (Percent)
0-1	10.9%	85.3%	3.8%
1-2	15.1	79.3	5.6
2-3	20.5	74.7	4.8
5-6	14.4	83.7	1.9
10-11	8.2	91.6	.2
11.3-12.3	.3	99.7	--

Table 5-6: Comparison Between Energy Absorbed from Nuclear and Ionization Collisions and Energy lost by Leakage in Each of Six Inner Volumes.

Of the 2000 incident protons, about 140 (7%) remained in the one square millimeter beam cross section for the entire penetration path. About 1180 (59%) remained in a one square centimeter volume centered on the Z-axis. Another 322 (16%) of the protons were scattered out of the 1 x 1 x 12.3 cm^3 volume. The remaining 498 (25%) had nuclear reactions. The distribution of secondaries is given in Table 5-1. The secondary neutrons rarely produced events in the central 1 x 1 x 12.3 cm^3 core. Most of the secondary protons were also scattered out.

In the 0-1 cubic cm volume, the major portion of the protons are still within the beam dimensions. The suitable dose volume for the absorption of the 19,205 MeV is .1 x .1 x 1 cm^3. In the final inner volume, most of the 1180 remaining protons are distributed throughout the 1 x 1 x 1 cm^3 and this is the suitable volume for the dose calculation. The PROPER 3B system permits the user to select the exact volume for the calculation. For the example given here, the chosen dose volume can be any inner volume and have any size which fits the parameters of the problem. In addition to the total energy, the user may select any energy bands of interest and can study in detail the nuclear and ionization energy distributions of as many different inner volumes, both on and off the central beam path, as required by the problem.

CHAPTER 6

Lateral leakage of protons from silicon rods bombarded by monoenergetic protons in the energy range 50 MeV - 187 MeV

by Martin Leimdorfer

Introduction

In connection with a study of the properties of lithium-drifted silicon semiconductor detectors a calculation has been made to investigate the lateral leakage rate and the leaking particle spectrum. The silicon absorbers were assumed to be cylindrical rods of circular cross section. The source particles were assumed to enter uniformly over a circular area, concentric with an end surface of the absorber. The radius of this area was varied. The theoretical treatment is based on a Monte Carlo method, previously described [1]. The PROTOS computer program, which was used, was altered to incorporate a treatment of nuclear interactions according to a model described in [2]. Only protons coming out directly from a nuclear interaction were considered and no attempt was made to take into account the secondary generations of protons produced via intermediary neutrons colliding with nuclei. The nuclear interaction treatment in this study is only meant to provide a basis for general observations of tendencies in the effects and is rather approximate. However, in order to show, explicitly, the influence of nuclear interactions upon the present results, calculations were made with as well as without nuclear interactions.

Energy step density in the Monte Carlo calculation, comparisons with analytical model

The Monte Carlo procedure uses a grid of energy points which are generally equally spaced in the logarithm of the energy between the source energy and a cutoff energy which is chosen so that all particles are essentially stopped as far as their spatial movement is concerned. This cutoff energy was set to 2 MeV in all cases of this study. In order to treat the proton slowing down process correctly, the energy

grid has to be sufficiently dense to provide numerically converged results. An exploratory study was made to check this effect at 187 MeV source energy. An analytical model (see Appendix I) was also developed to produce a formula that can be used for hand calculations of the total leakage rate. The advantage of this model in the present context is, of course, that it can also be used to check whether the results are, indeed, converged as far as the energy mesh density of the Monte Carlo calculation is concerned.

In table I we shall compare results of calculations made with 100-point and 50-point logarithmic grids as well as 16-point linear grids. The geometries correspond to four different cases: In the first three cases the cross section areas of the absorbers were 9, 25, and 100 mm^2, respectively and the source area was 1 mm^2. In the fourth case both the absorber area and the source area were 9 mm^2. Results with as well as without nuclear interactions are displayed. The lengths of the absorbers were always longer than the range of the source particles. The direction of the source protons is along the axis of the cylindrical absorber throughout this set of calculations.

Table I

Total leakage rates (per cent) at various energy grid densities in the Monte Carlo calculation and as obtained from analytical model

Energy spacing	Absorber/source cross section areas			
	9 mm^2/1 mm^2	25 mm^2/1 mm^2	100 mm^2/1 mm^2	9 mm^2/9 mm^2
With nuclear interactions				
100-point log.	93.7 ± 2.2	81.3 ± 2.0	42.9 ± 1.5	95.4 ± 2.2
50-point log.	95.8 ± 2.2	82.4 ± 2.0	48.0 ± 1.6	96.7 ± 2.2
16-point linear	94.2 ± 2.2	83.1 ± 2.0	51.1 ± 1.6	95.7 ± 2.2
Without nuclear interactions				
100-point log.	95.0 ± 2.2	80.1 ± 2.0	40.0 ± 1.4	95.6 ± 2.2
50-point log.	95.4 ± 2.2	82.9 ± 2.0	43.2 ± 1.5	96.8 ± 2.2
Analytical results - no nuclear interactions				
	92.4	80.8	42.7	-

The errors indicated in the table refer to uncertainties corresponding to one standard deviation in the statistics. The analytical results are based on the assumption that the source is an infinitely narrow beam and that spatial straggling can be neglected. It is obvious, though, that the analytical results are quite accurate. Since computation times in the Monte Carlo cases are rather long (of the order of an hour per case) we decided to use a 50-point logarithmic grid for the bulk of the calculations at other source energies. The computation times are proportional to the number of energy points used. The results of the table indicate that the final choice of the 50-point grid density is acceptable from a point of view of accuracy.

Total lateral leakage rates

Monte Carlo calculations were performed at the source energies 50 MeV, 100 MeV, and 187 MeV respectively. In most of the calculations, the source beam was made thin enough to be considered as a line source. The results of total leakage rates as a function of the cross section area of the silicon absorbers are displayed in figs. 1 - 3. The source particles enter along the direction of the cylinder axis in all of these cases.

Fig. 1 shows the 187 MeV case (50-point grid). The inclusion of nuclear interactions in the calculations obviously does not affect the results appreciably. As seen in fig. 2, in the case of a 100 MeV source (50-point grid) the nuclear interactions influence the results to a much greater extent than in the previous case. This effect is even more pronounced in the case of a 50 MeV source, as shown in fig. 3. A probable explanation of this phenomenon could be that higher energy protons are so much deflected by Coulomb scattering as to make the effects of nuclear processes less observable in the quantities presented.

Variation of angle of incidence at 187 MeV

In all results given above the direction of the incident protons is along the axis of the absorbing cylinder. In order to facilitate comparisons with experiments performed at Uppsala University with a 187 MeV beam with varying directions of incidence relative to the axis of the absorbing cylinder we performed a study of this directional effect. The results of the total lateral leakage as a function of the angle of incidence of the source beam are displayed in Table II. A 50-MeV logarithmic grid was used throughout.

Table II

Lateral leakage (in per cent) for 187 MeV proton source and varying directions of incidence with respect to the axis of the absorbing cylinders

Beam angle (radians)	With nuclear interactions			
	Absorber/source cross section area			
	9 mm^2/1 mm^2	25 mm^2/1 mm^2	100 mm^2/1 mm^2	9 mm^2/9 mm^2
0	95.8 ± 2.2	82.4 ± 2.0	48.0 ± 1.6	96.7 ± 2.2
0.01	96.3 ± 2.2	84.6 ± 2.0	49.4 ± 1.6	97.9 ± 2.2
0.02	96.8 ± 2.2	86.9 ± 2.0	54.4 ± 1.6	99.9 ± 2.2

Energy spectra of protons leaking laterally

In all the calculational cases described above, energy distributions of the protons, leaking out laterally, were also obtained as part of the computer results. In the present report we shall give results for 187 MeV source protons incident axially. Table III shows these results. The unit is number of escaping protons per MeV per source proton. A 50-point logarithmic energy grid was used in these calculations. Fig. 4 shows a plot of the results for the 25 mm^2 absorber with as well as without nuclear interactions. Fig. 5 shows an approximate curve fit on a linear graph of the results given in fig. 4. As seen, the nuclear interactions result in a pile-up of low-energy protons whereas the spectrum neglecting these processes is essentially cut off at around 30 MeV.

Translation of leakage spectrum to detector response function

It is now appropriate to discuss the problem of how a calculated leakage spectrum can be used to make a prediction of the detector response function, i.e. the pulseheight distribution, recorded from a detector having a sensitive volume of the shape of the absorbers used in our calculations. Let us assume, first, that nuclear interactions are not occurring in nature. In that case each source particle will deposit an energy in the absorber amounting to its initial energy minus that of any single particle escaping. Hence, the distribution of energy deposition is readily obtained by changing the values on the abscissa of the leakage spectrum from their previous values to new values equal to the source energy minus the previous abscissa value. The existence of nuclear interactions distort this simple picture, however. In a nuclear interaction, in the energy range considered here, the kinetic energy

of the incoming particle is transferred to kinetic energies of the reaction products (plus minor potential energies due to non-conservation of mass in the reaction). The outgoing nucleons will carry practically all the kinetic energy available since they are the lightest ones of the reaction products. The number of outgoing nucleons will practically always be different from one. In a typical case of, say, a 100 MeV proton incident on a silicon nucleus there will be on the average about 1.2 high-energy (100 MeV - 25 MeV) protons and about 0.8 high-energy neutrons plus roughly 0.5 low-energy (25 MeV - 0) neutrons and protons, respectively. The high-energy particles are generally called cascade particles and the low-energy particles are called evaporation particles, following the theoretical model used to predict the outcome of such nuclear reactions. In the present context it is important that we note that the low-energy reaction products are always accompanied by high-energy particles, emitted at essentially the same time. This means that the detector will not record pulses corresponding to energy escapes seen in the low-energy peak of the nuclear interaction escape spectrum of fig. 4 or 5 (there is one very improbable exception, namely, if the kinetic energy of the incoming particle is transferred to one low-energy proton and one or more neutrons).

It is clear now that there is no way to derive, in a simple manner, the probability distribution of energy deposited in the sensitive volume of the detector from the leakage spectra displayed in the present report. Since, however, the latter spectra for 187 MeV incident protons, are quite similar in the cases with and without nuclear interactions, respectively, (apart from the region of very low energies, in which case the nuclear interaction products can not be distinguished by the detector because of the pile-up effect, discussed above) it is still likely that a comparison with experiments, based on the abscissa reflection procedure, discussed above, will show reasonable agreement between theory and experiment at this source energy.

It is, of course, very simple to make the computer program calculate the actual distributions of absorbed energy. This will be done in the very near future when the new PROTOS 3 program will be available with the final set of nuclear interaction data. In this case, contributions from multiple neutron-proton interaction chains as well as from heavier particles than nucleons will also be considered, even though one may expect that these will not be substantial.

Table III

Energy distributions of protons leaking laterally

Energy group (MeV)	With nuclear interactions				Without nuclear interactions			
	Absorber/source cross section area (mm^2)				Absorber/source cross section area (mm^2)			
	9/1	25/1	100/1	9/9	9/1	25/1	100/1	9/9
187.00 - 170.46	2.72E-4	0	0	9.16E-3	4.83E-4	0	0	1.05E-2
170.46 - 155.38	7.13E-3	3.65E-4	0	1.21E-2	6.67E-3	2.32E-4	0	1.23E-2
155.38 - 141.64	1.38E-2	3.49E-3	0	1.04E-2	1.50E-2	4.51E-3	0	1.17E-2
141.64 - 129.11	1.34E-2	9.26E-3	3.59E-4	8.50E-3	1.58E-2	8.46E-3	1.60E-4	1.04E-2
129.11 - 117.69	1.06E-2	9.85E-3	1.14E-3	7.74E-3	1.01E-2	1.13E-2	1.23E-3	7.27E-3
117.69 - 107.28	7.1[illegible]E-3	9.80E-3	2.40E-3	4.80E-3	8.41E-3	1.10E-2	2.69E-3	5.72E-3
107.28 - 97.79	5.27E-3	8.17E-3	3.95E-3	4.00E-3	6.01E-3	9.59E-3	3.69E-3	4.69E-3
97.79 - 89.14	4.39E-3	6.65E-3	5.09E-3	3.64E-3	5.84E-3	7.98E-3	4.91E-3	3.82E-3
89.14 - 81.26	3.55E-3	5.90E-3	4.31E-3	2.28E-3	4.25E-3	7.04E-3	6.60E-3	3.30E-3
81.26 - 74.07	3.20E-3	4.52E-3	5.84E-3	2.37E-3	3.27E-3	5.50E-3	5.43E-3	2.09E-3
74.07 - 67.52	2.82E-3	5.27E-3	5.65E-3	3.05E-3	1.83E-3	3.51E-3	5.19E-3	1.83E-3
67.52 - 61.55	2.43E-3	4.19E-3	5.44E-3	2.01E-3	1.84E-3	4.86E-3	6.78E-3	1.59E-3
61.55 - 56.10	1.84E-3	4.41E-3	5.79E-3	2.94E-3	1.29E-3	3.86E-3	4.96E-3	1.56E-3
56.10 - 51.14	2.02E-3	3.22E-3	5.34E-3	1.11E-3	2.32E-3	3.33E-3	4.33E-3	1.31E-3
51.14 - 46.62	1.99E-3	3.21E-3	4.97E-3	1.88E-3	8.84E-4	3.32E-3	4.75E-3	1.33E-3
46.62 - 42.49	1.33E-3	3.40E-3	2.91E-3	1.21E-3	1.70E-3	2.79E-3	3.88E-3	8.49E-4
42.49 - 38.73	1.60E-3	2.79E-3	4.66E-3	9.31E-4	7.98E-4	1.86E-3	2.93E-3	3.99E-4
38.73 - 35.31	2.63E-3	3.21E-3	3.79E-3	1.61E-3	5.84E-4	2.19E-3	3.36E-3	7.30E-4
35.31 - 32.18	8.00E-4	1.92E-3	4.00E-3	1.28E-3	1.28E-3	2.72E-3	2.40E-3	3.20E-4
32.18 - 29.34	2.11E-3	2.28E-3	2.63E-3	1.58E-3	5.27E-4	1.76E-3	3.34E-3	7.03E-4
29.34 - 26.74	1.54E-3	1.35E-3	4.82E-3	1.35E-3	5.78E-4	2.50E-3	2.31E-3	5.78E-4
26.74 - 24.38	2.33E-3	1.06E-3	1.69E-3	1.48E-3	2.11E-3	4.27E-4	1.90E-3	6.34E-4
24.38 - 22.22	1.16E-3	1.62E-3	1.86E-3	2.32E-4	0	6.96E-4	1.16E-3	2.32E-4
22.22 - 20.26	1.02E-3	2.04E-3	2.04E-3	7.64E-4	5.09E-4	7.63E-4	1.02E-3	2.54E-4
20.26 - 18.46	1.12E-3	1.40E-3	2.23E-3	1.12E-4	5.58E-4	8.37E-4	2.79E-4	0
18.46 - 16.83	1.22E-3	9.18E-4	1.53E-3	9.18E-4	0	3.06E-4	9.18E-4	
16.83 - 15.34	1.01E-3	1.01E-3	1.34E-3	6.72E-4		3.36E-4	3.36E-4	
15.34 - 13.99	3.68E-4	1.47E-3	1.11E-3	2.21E-3		3.68E-4	3.37E-4	
13.99 - 12.75	1.62E-3	3.23E-3	2.02E-3	2.02		0	0	
12.75 - 11.62	2.22E-3	1.33E-3	4.43E-4	4.43E-4		0	4.43E-4	
11.62 - 10.59	1.95E-3	2.43E-3	2.92E-3	2.92E-3		4.86E-4	4.86E-4	
10.59 - 9.66	2.13E-3	1.60E-3	3.20E-3	4.80E-3		0	5.34E-4	
9.66 - 8.80	2.43E-3	2.34E-3	2.93E-3	1.76E-3		0	0	
8.80 - 8.02	1.28E-3	4.50E-3	2.57E-3	3.21E-3		0		
8.02 - 7.31	4.23E-3	2.11E-3	3.52E-3	3.52E-3		0		
7.31 - 6.67	3.86E-3	3.86E-3	7.73E-3	1.55E-3		0		
6.67 - 6.08	1.70E-3	2.54E-3	2.54E-3	5.09E-3		0		
6.08 - 5.54	5.58E-3	2.79E-3	2.79E-3	2.79E-3		9.30E-4		
5.54 - 5.05	1.02E-3	6.12E-3	2.04E-3	7.14E-3		0		
5.05 - 4.60	6.72E-3	3.36E-3	5.60E-3	1.12E-3				
4.60 - 4.20	7.37E-3	3.68E-3	4.91E-3	7.37E-3				
4.20 - 3.82	4.04E-3	6.74E-3	5.39E-3	5.39E-3				
3.82 - 3.49	4.43E-3	1.03E-2	0	4.43E-3				
3.49 - 3.18	3.24E-3	4.86E-3	0	3.24E-3				
3.18 - 2.90	7.12E-3	7.12E-3	1.78E-3	3.56E-3				
2.90 - 2.64	1.37E-2	1.95E-3	5.85E-3	5.85E-3				
2.64 - 2.41	1.07E-2	1.50E-2	4.28E-3	6.42E-3				
2.41 - 2.19	4.70E-3	2.35E-3	0	9.39E-3				
2.19 - 2.00	1.29E-2	5.15E-3	7.73E-3	2.58E-3	0	0	0	0

Appendix I

An analytical representation of the total lateral leakage fraction

Assume that charged particles are incident along a normal to a slab of infinite extension. Using the theory of Eyges [3] one may derive an expression for the distribution in distance from the source normal of particles transmitted through the slab. Eyges' theory neglects range straggling and assumes the validity of the small-angle diffusion approximation of the multiple scattering transport equation. Denoting the Eyges normalized distribution $f(r) \cdot 2\pi r dr$ we may obtain an expression for the total lateral leakage fraction for a cylinder of radius R

$$L = \int_R^\infty f(r) \cdot 2\pi r dr$$

where we have assumed that particles transmitted at $r \geq R$ in the slab problem would have escaped through the lateral surface in the cylinder problem.

Taking Eyges' expression for f(r) we obtain

$$f(r) = \frac{1}{2\pi\sigma} e^{-\frac{r^2}{2\sigma^2}}$$

In deriving this formula we have tacitly assumed that the gaussian distribution projected on a plane through the axis of incidence will also be valid for the unprojected distribution in r. This is a known feature of the normal distribution.

The result for the lateral leakage fraction is

$$L = e^{-\frac{R^2}{2\sigma^2}}$$

where

$$\sigma^2 = \tfrac{1}{2} \int_0^X \theta_s^2 (X-x)^2 \, dx$$

X being the thickness of the absorber measured along the line of incidence and θ_s^2 the rate of change of the mean square of the particle deflection angle. We take an expression for θ_s^2 from Rossi [4]

$$\theta_s^2 = 16\pi N\frac{Z^2}{A} r_e^2 \left(\frac{m_o}{\beta p}\right)^2 \ln\left[196Z^{-1/3}\left(\frac{Z}{A}\right)^{1/6}\right]$$

where

N is Avogadro's number

Z is the atomic number of the absorber nucleus

A " " " weight " " " "

r_e is the classical radius of the electron

m_o is the mass of the electron

c is the velocity of light

β is the ratio of the particle velocity and the velocity of light

p is the particle momentum

In using the Rossi expression for θ_s^2 we neglect the effect of range straggling and transform the quantities β and p into deterministic functions of the variable penetration distance x. This is done by first turning β and p into functions of the particle kinetic energy E which is a function of x through the equation

$$x = \int_E^{E_o} -\frac{dE}{\left(\frac{dE}{dx}\right)}$$

where E_o is the source energy and $\frac{dE}{dx}$ the stopping power which is available in standard handbooks. We took this quantity from our own calculations based on the Bethe-Block formula with a mean ionization potential for silicon equal to 123 eV.

The final value of σ^2 arrived at by numerical integration for 187 MeV protons incident on silicon was 1.00 $(g/cm^2)^2$. In Table IV we compare the analytical values of the lateral leakage fraction with the best values of the corresponding computations (100-point grid, no nuclear interactions).

Table IV

Comparison of analytical and Monte Carlo results of lateral leakage at 187 MeV (per cent)

Absorber cross section area (mm^2)	Lateral leakage	
	Analytical	Monte Carlo
9	92.4	95.0 ± 2.2
25	80.8	80.1 ± 2.0
100	42.7	40.0 ± 1.5

It is obvious that the analytical values are in good agreement with those obtained by the Monte Carlo method.

References:

[1] C. Johansson and M. Leimdorfer: "Description of the Theoretical Background for PROTOS 3". Chapter 3, this volume.

[2] M. Leimdorfer, J. Barish: "A Method of Representing Two-Dimensional Distributions for Use in Monte Carlo Calculations". ORNL-4002 (1967).

[3] L. Eyges: "Multiple Scattering with Energy Loss". Phys. Rev. 74 (1958) 1534.

[4] B. Rossi: "High-Energy Particles". Prentice-Hall Inc. (1952) 67.

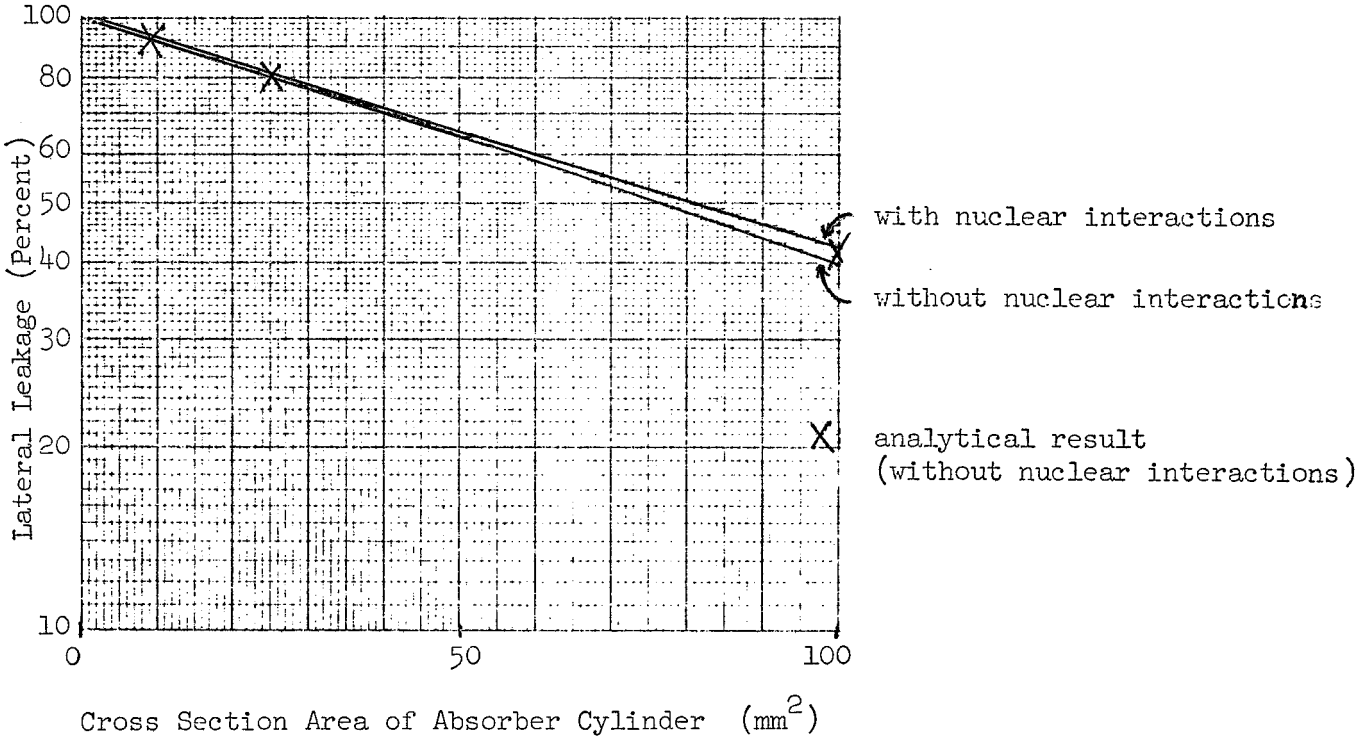

Figure 6-1. Lateral Leakage Fraction as a Function of Cross Section Area

Source Energy: 187 MeV. Line Source.

Curves represent Monte Carlo results with a 100-point grid.
Crosses are analytical results obtained by the method described in Appendix I.

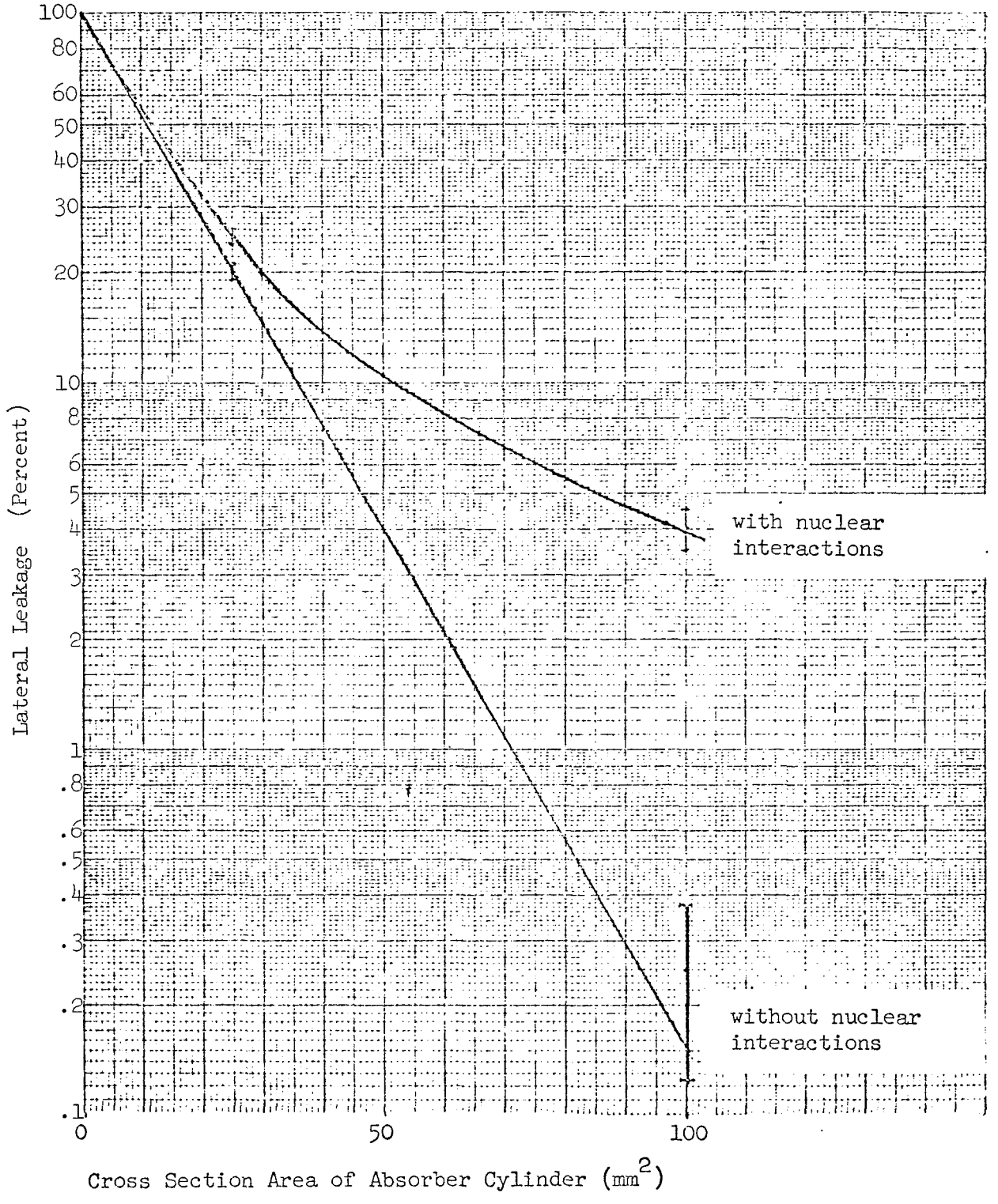

Figure 6-2. Lateral Leakage Fraction as a Function of Cross Section Area

Source Energy: 100 MeV. Line Source.
Curves represent Monte Carlo results with a 50-point energy grid.
Error bars correspond to one standard deviation.

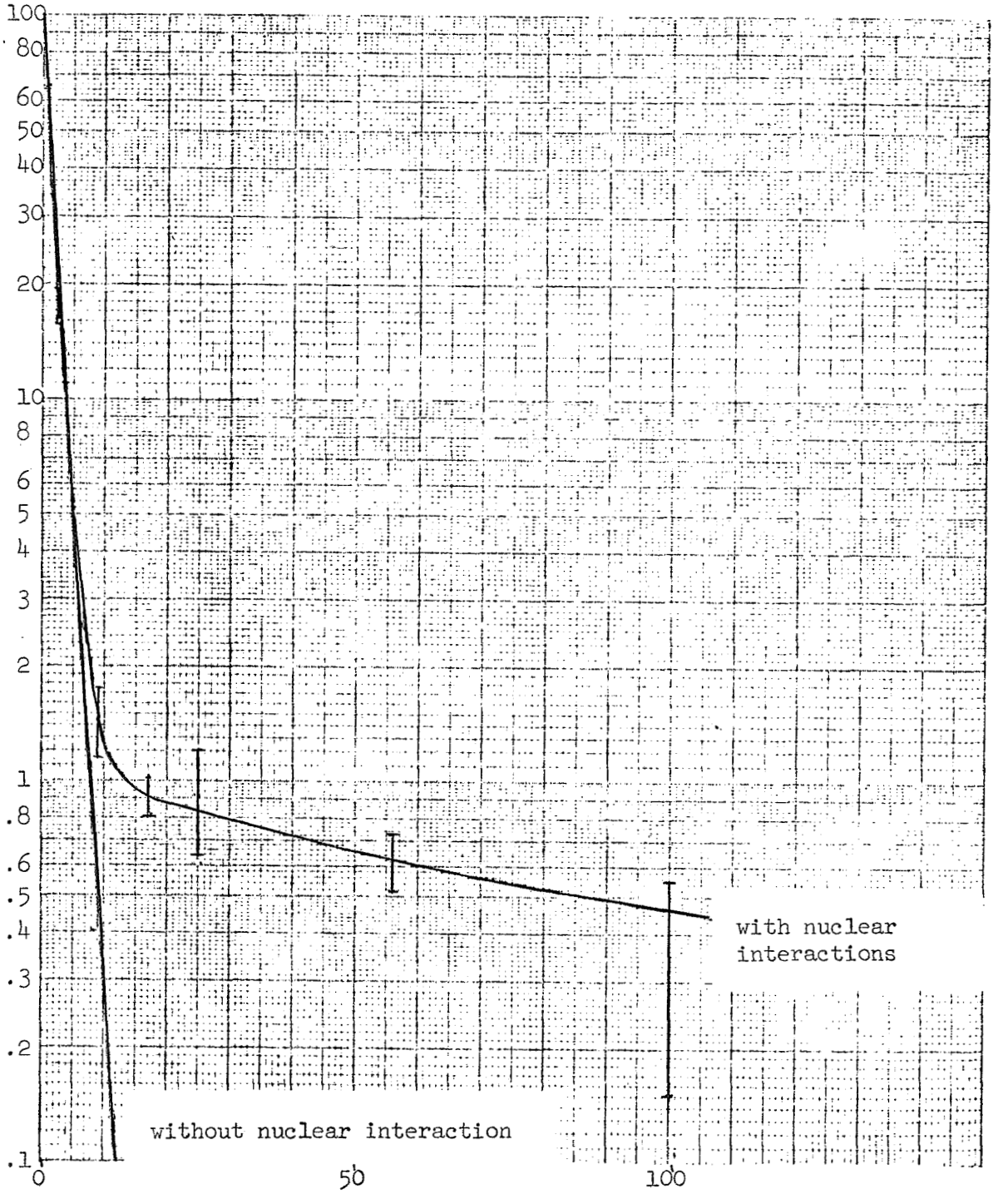

Figure 6-3: Lateral Leakage Fraction as a Function of Cross Section Area

Source Energy: 50 MeV. Line Source.

Curves represent Monte Carlo results with a 50-point energy grid.
Error bars correspond to one standard deviation.

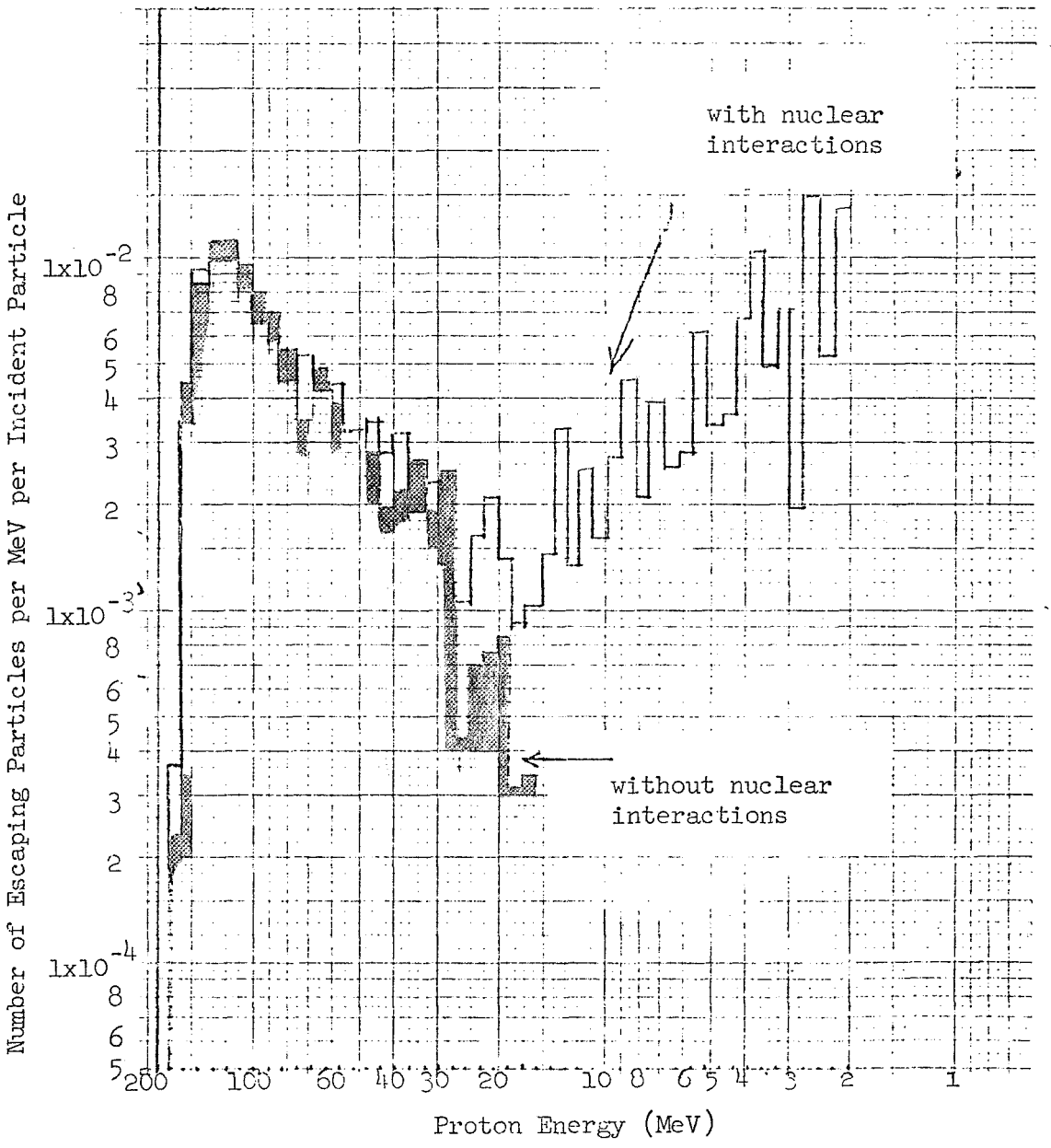

Figure 4: Energy Distributions of Protons Escaping Laterally from Absorber with 25 mm^2 cross section Area.

Shaded histogram represents the case without nuclear interactions.
50-point energy grid. Line source.

Figure 5: Approximate Curve Fit to Histogram Results of Figure 4.